

HYDRAULIC MODELLING OF PURGING
IN SEA OUTFALL

CENTRE FOR NEWFOUNDLAND STUDIES

**TOTAL OF 10 PAGES ONLY
MAY BE XEROXED**

(Without Author's Permission)

SUNARYO



**HYDRAULIC MODELLING OF PURGING
IN SEA OUTFALL**

By

OSUNARYO

**A Thesis Submitted to the School of Graduate Studies
in Partial Fulfilment of the Requirements for
the Degree of Master of Engineering**

**FACULTY OF ENGINEERING AND APPLIED SCIENCE
MEMORIAL UNIVERSITY OF NEWFOUNDLAND
AUGUST 1994
ST JOHN'S NEWFOUNDLAND CANADA**



National Library
of Canada

Acquisitions and
Bibliographic Services Branch

395 Wellington Street
Ottawa, Ontario
K1A 0N4

Bibliothèque nationale
du Canada

Direction des acquisitions et
des services bibliographiques

395, rue Wellington
Ottawa (Ontario)
K1A 0N4

Your slip *Votre référence*

Our file *Notre référence*

The author has granted an irrevocable non-exclusive licence allowing the National Library of Canada to reproduce, loan, distribute or sell copies of his/her thesis by any means and in any form or format, making this thesis available to interested persons.

L'auteur a accordé une licence irrévocable et non exclusive permettant à la Bibliothèque nationale du Canada de reproduire, prêter, distribuer ou vendre des copies de sa thèse de quelque manière et sous quelque forme que ce soit pour mettre des exemplaires de cette thèse à la disposition des personnes intéressées.

The author retains ownership of the copyright in his/her thesis. Neither the thesis nor substantial extracts from it may be printed or otherwise reproduced without his/her permission.

L'auteur conserve la propriété du droit d'auteur qui protège sa thèse. Ni la thèse ni des extraits substantiels de celle-ci ne doivent être imprimés ou autrement reproduits sans son autorisation.

ISBN 0-612-13952-2

Canada



To :

My mother Dasiyah

My parents in law Dr. Darfioes Basir and Yunifah

My wife Venny Darti

My daughters Hanna Khairat and Shelleza Sholihah



Abstract

The presence of seawater in a sea outfall can reduce the effluent discharge from a land-based treatment plant or domestic and industrial areas. In the longterm, it can damage the sea outfall. To avoid the presence of seawater and to anticipate a varying effluent discharge, a minimum effluent discharge is needed to purge the outfall system.

The objective of this study was to investigate various ways of decreasing the minimum effluent discharge needed to purge a sea outfall. The effect of port size and an increase in mixing between saltwater and effluent are considered in this study. In tests on the effect of port size, three different types of tests were undertaken. There included risers without caps, risers with caps having one port of diameter 2.54 cm (one inch), and risers with caps having two ports of diameter 2.54 cm (one inch). Attempts were made to increase mixing in the vertical risers using small water jets located below the risers, water jets located upstream of the risers, air jets located below the risers and a barrier located at the top of tunnel upstream the risers.

The maximum reduction in the purging discharge was obtained using water jets (1.00 l/min) located below all risers. The purging discharge using these jets was only 48% of that without water jets. This is a significant reduction.

Acknowledgements

The author would like to express great appreciation to Dr. James J. Sharp for his guidance, advice, support and encouragement during the experiment until the completion of this thesis.

I also gratefully acknowledge the Government of Indonesia and the Canadian International Development Agency (CIDA) for providing financial support, and Memorial University of Newfoundland, the School of Graduate Studies and the Faculty of Engineering and Applied Science for their support during my study.

Further, I would like to thank Dr. Leonard Lye, P. Eng. the Project Leader of the CIDA/DPU Professional Development Project, Memorial University of Newfoundland.

I would like also to thank to the Natural Sciences and Engineering Research Council of Canada for financial support to prepare all the materials of the experiment, and Darryl who helped me complete the experiment.

Finally, I would like to extend my appreciation and thanks to my wife Venny Darti, my daughters Hanna Khairat and Shelleza Sholihah, my mother Dasiyah, and my parents in law Dr. Darfioes Basir and Yunifah for their love, patience, sacrifices, and understanding.

Table of Contents

Abstract	iii
Acknowledgement	iv
Table of Contents	v
List of Tables	viii
List of Figures	ix
List of Symbols	xv
Chapter 1 Introduction	1
1.1. Sea outfalls as delivery of effluents to ocean	1
1.2. Sea outfalls for Indonesia	3
1.3. Objective of this study	4
Chapter 2 Literature Review	6
2.1. Jet, plume, and buoyant jet	6
2.1.1. General	6
2.1.2. Jet	7
2.1.3. Plume	10
2.1.4. Buoyant jet	13
2.1.4.1. Horizontal buoyant jet	13
2.1.4.2. Vertical buoyant jet	18
2.2. Dilution	22

2.2.1. Initial dilution	23
2.2.2. Secondary dilution	32
2.2.3. Bacterial decay	37
2.3. Saline intrusion and purging in sea outfalls	39
2.3.1. Saline intrusion	39
2.3.2. Purging	44
2.4. Prevention of seawater intrusion	48
Chapter 3 Laboratory Study	52
3.1. Purpose and general outline of study	52
3.2. Experimental facilities	53
3.3. Experimental procedure	60
3.3.1. General	60
3.3.2. Saltwater preparation	63
3.3.3. Test procedure	65
3.3.4. Recording of result	75
Chapter 4 Results and Discussion	79
4.1. General	79
4.2. Tests on the effect of port size	80
4.3. Tests on jets and barrier	92
4.3.1. Tests using water jets	92
4.3.1.1. Water jets located below risers	96
4.3.1.2. Water jet located upstream of risers	99

4.3.2. Tests using air jets	100
4.3.3. Test using a barrier	100
Chapter 5 Conclusions and Recommendations	102
5.1. Conclusions	102
5.2. Recommendations	104
References	105
Appendix A Saline wedge profiles in tunnel with risers without caps	A.0
Appendix B Saline wedge profiles in tunnel for different types of test	B.0

List of Tables

Table No.	Page No.
3.1. Summary of the test procedures	76
4.1. Data collected on three types of test	83
4.2. Analysis of data collected on three types of test	83
4.3. Condition of flow in riser # 1 at same freshwater discharge and density for different numbers of caps and ports	90
4.4. Condition of flow in riser # 2 at same freshwater discharge and density for different numbers of caps and ports	90
4.5. Condition of flow in riser # 3 at same freshwater discharge and density for different numbers of caps and ports	91
4.6. Condition of flow in riser # 4 at same freshwater discharge and density for different numbers of caps and ports	91
4.7. Condition of flow in riser # 1 at same freshwater discharge and density for different types of test	94
4.8. Condition of flow in riser # 2 at same freshwater discharge and density for different types of test	95
4.9. Condition of flow in riser # 3 at same freshwater discharge and density for different types of test	96
4.10. Condition of flow in riser # 4 at same freshwater discharge and density for different types of test	98

List of Figures

Figure No.	Page No.
1.1. Schematic diagram of sea outfall	2
1.2. Location of capital cities of Provinces in Indonesia	5
2.1. Zone of flow establishment (ZFE) and zone of established flow (ZEF) (Albertson et al., 1950)	7
2.2. Cross sectional profile of a buoyant jet (Abraham, 1963)	14
2.3. Parameters of flow involved in theoretical analysis of buoyant plume (Morton et al., 1956)	20
2.4. Initial dilution after Rawn, Bowerman and Brooks (1960)	24
2.5. Generalised chart of various workers for surface dilution of a buoyant jet (Liseth, 1970)	27
2.6. Effluent discharge from sea outfall at various stages of purging	45
2.7. a. An intrusion proof diffuser, b. An intrusion proof head, c. Anti- intrusion flexible 'duck-bill' valve, d. A venturi shaped outlet port, and e. A cranked tunnel-diffuser (Charlton, 1985a)	50
2.8. a. Venturi control Mk I-circular section, asymmetric (Charlton, 1985b) and b. Venturi control Mk II-vertical sided (Charlton, 1985b)	51
3.1. Photograph of the experimental facilities	54
3.2. Experimental facilities	55

Figure No.	Page No.
3.3. Photograph of the flowmeters model # 10A3555A	57
3.4. Photograph of the flowmeters model # 10A6731N	58
3.5. Photograph of the flowmeter model # FP-1/2-21-G-10/77	59
3.6. a. Risers with no caps; b. Risers with caps, each with two ports; and c. Risers with caps, each with one port	62
3.7. a. Water jets located below risers; b. Water jet located upstream risers; c. Air jets located below risers; and d. Top barrier located upstream risers	64
3.8. Schematic of saltwater preparation	66
3.9. Schematic of the experiment with water jets located below the risers in the tunnel	71
3.10. Schematic of the experiment with water jet located upstream the risers in the tunnel	72
3.11. Schematic of the experiment with air jets located below the risers in the tunnel	73
3.12. Schematic of the air bubble measuring	74
3.13. Recording procedures, a. Front view, and b. Plan view	78
3.14. Typical set of three photographs	79
4.1. Port densimetric Froude number as a function of tunnel diameter to port diameter	85

4.2. Port densimetric Froude number as a function of riser height to port diameter	86
4.3. Critical densimetric Froude number as a function of tunnel diameter to port diameter	87
A.1. Saline wedge profile in tunnel with riser without caps at effluent discharge $Q = 11.36$ l/min and $\Delta\rho = 0.010$ g/cm ³	A.1
A.2. Saline wedge profile in tunnel with riser without caps at effluent discharge $Q = 28.39$ l/min and $\Delta\rho = 0.010$ g/cm ³	A.1
A.3. Saline wedge profile in tunnel with riser without caps at effluent discharge $Q = 36.34$ l/min and $\Delta\rho = 0.010$ g/cm ³	A.1
A.4. Saline wedge profile in tunnel with riser without caps at effluent discharge $Q = 39.75$ l/min and $\Delta\rho = 0.010$ g/cm ³	A.2
A.5. Saline wedge profile in tunnel with riser without caps at effluent discharge $Q = 54.51$ l/min and $\Delta\rho = 0.010$ g/cm ³	A.2
A.6. Saline wedge profile in tunnel with riser without caps at effluent discharge $Q = 68.14$ l/min and $\Delta\rho = 0.010$ g/cm ³	A.2
A.7. Saline wedge profile in tunnel with riser without caps at effluent discharge $Q = 76.08$ l/min and $\Delta\rho = 0.010$ g/cm ³	A.3
B.1. Saline wedge profiles in tunnel with risers without caps at different freshwater discharges, and $\Delta\rho = 0.010$ g/cm ³	B.1

- B.2. Saline wedge profiles in tunnel with risers without caps at different freshwater discharges, and $\Delta\rho = 0.020 \text{ g/cm}^3$ B.1
- B.3. Saline wedge profiles in tunnel with risers having caps with two ports at different freshwater discharges, and $\Delta\rho = 0.020 \text{ g/cm}^3$ B.2
- B.4. Saline wedge profiles in tunnel with risers having caps with one port at different freshwater discharges, and $\Delta\rho = 0.020 \text{ g/cm}^3$ B.2
- B.5. Saline wedge profiles in tunnel with water jet located at first riser ($Q_{21} = 1.00 \text{ l/min}$), at different freshwater discharges, and $\Delta\rho = 0.010 \text{ g/cm}^3$... B.3
- B.6. Saline wedge profiles in tunnel with water jet located at second riser ($Q_{22} = 1.00 \text{ l/min}$), at different freshwater discharges, and $\Delta\rho = 0.010 \text{ g/cm}^3$. B.3
- B.7. Saline wedge profiles in tunnel with water jet located at third riser ($Q_{23} = 1.00 \text{ l/min}$), at different freshwater discharges, and $\Delta\rho = 0.010 \text{ g/cm}^3$. B.4
- B.8. Saline wedge profiles in tunnel with water jet located at fourth riser ($Q_{24} = 1.00 \text{ l/min}$), at different freshwater discharges, and $\Delta\rho = 0.010 \text{ g/cm}^3$... B.4
- B.9. Saline wedge profiles in tunnel with water jets located at first and second risers ($Q_{21} = Q_{22} = 1.00 \text{ l/min}$), at different freshwater discharges, and $\Delta\rho = 0.010 \text{ g/cm}^3$ B.5
- B.10. Saline wedge profiles in tunnel with water jets located at second and third risers ($Q_{22} = Q_{23} = 1.00 \text{ l/min}$), at different freshwater discharges, and $\Delta\rho = 0.010 \text{ g/cm}^3$ B.5

- B.11. Saline wedge profiles in tunnel with water jets located at third and fourth risers ($Q_{23} = Q_{24} = 1.00$ l/min), at different freshwater discharges, and $\Delta\rho = 0.010$ g/cm³ B.6
- B.12. Saline wedge profiles in tunnel with water jets located at first, second and third risers ($Q_{21} = Q_{22} = Q_{23} = 1.00$ l/min), at different freshwater discharges, and $\Delta\rho = 0.010$ g/cm³ B.6
- B.13. Saline wedge profiles in tunnel with water jets located at second, third and fourth risers ($Q_{22} = Q_{23} = Q_{24} = 1.00$ l/min), at different freshwater discharges, and $\Delta\rho = 0.010$ g/cm³ B.7
- B.14. Saline wedge profiles in tunnel with water jets located at first, second, third and fourth risers ($Q_{21} = Q_{22} = Q_{23} = Q_{24} = 1.00$ l/min), at different freshwater discharges, and $\Delta\rho = 0.010$ g/cm³ B.7
- B.15. Saline wedge profiles in tunnel with water jet located upstream of first riser ($Q_{25} = 1.00$ l/min), at different freshwater discharges, $L_1 = 508$ mm, and $\Delta\rho = 0.010$ g/cm³ B.8
- B.16. Saline wedge profiles in tunnel with water jet located upstream of first riser ($Q_{25} = 1.00$ l/min), at different freshwater discharges, $L_1 = 762$ mm, and $\Delta\rho = 0.010$ g/cm³ B.8
- B.17. Saline wedge profiles in tunnel with water jet located upstream of first riser ($Q_{25} = 1.00$ l/min), at different freshwater discharges, $L_1 = 1524$ mm, and $\Delta\rho = 0.010$ g/cm³ B.9

- B.18. Saline wedge profiles in tunnel with air jets located at first, second, third and fourth risers ($Q_{21} = 0.025$ l/min, $Q_{22} = 0.026$ l/min, $Q_{23} = 0.028$ l/min, and $Q_{24} = 0.028$ l/min), at different freshwater discharges, and $\Delta\rho = 0.010$ g/cm³ B.10
- B.19. Saline wedge profiles in tunnel with top barrier located upstream of first riser at different freshwater discharges, and $\Delta\rho = 0.010$ g/cm³ B.10

List of Symbols

Symbol	Description
A	the initial cross sectional area of jet the cross-sectional area of tunnel
B	the initial specific buoyancy flux of jet
C	the mass concentration of diffusing solute
C_m	the time-averaged maximum tracer concentration the centerline concentration of jet
C_{max}	the centerline concentration after travel time t
C_w	the waste concentration after the establishment of the waste field but before further diffusion
	the concentration of jet at port the initial coliform concentration
C_r	the concentration at a distance r from centerline of jet
C_t	the coliform concentration after time t
C_1	the dilution constants for the buoyancy dominated near field (BDNF)
C_2	the dilution constant for the buoyancy dominated far field (BDFF)
\bar{C}	the centerline concentration of jet at a distance z from port
CF	a correction factor
D	the diameter of pipe the diameter of tunnel

	the diffusion coefficient
F_c	the critical outfall densimetric Froude number
F_p	the densimetric Froude number at port
Fr_o	the densimetric Froude number at origin
F_d	a densimetric Froude number
H	the depth of jet discharge below surface
H_w	the height of wave
K	a numerical constant
K_{ps}, K_{pb}, K_{pc}	a jet coefficient
K_{ps}, K_{pb}, K_{pd}	a plume coefficient
L	the length of patch
L_o	the length of a saline wedge
	the length of an arrested wedge
L_w	the wave length
M	the initial specific momentum flux of jet
Q	the initial volume flux of jet
	the initial discharge of jet
	the volume flux of jet discharge
	the effluent flow required to purge outfall
Q_c	the critical effluent discharge required to purging of outfall
R_e	a Reynolds number
Re_d	a densimetric Reynolds numbers

R_o	a jet Richardson number
S	a centerline dilution a minimum surface dilution an average surface dilution without waves
S_b	the dilution due to die-off or disappearance of coliform bacteria
S_d	a secondary dilution
S_o	an initial dilution the dilution of jet fluid the still water dilution under identical conditions of depth and density difference
S_m	a minimum centerline dilution at surface a moving water dilution
S_w	an average surface dilution with waves
T_w	the wave period
T_{90}	the time required for 90% reduction in coliform concentration the time taken for 90% decay
U	the velocity of diffusion in the x direction
U_a	the velocity of ambient current
U_j	the velocity of jet at outfall
U_m	the velocity of the jet centerline
U_{max}	the maximum horizontal wave-induced velocity at discharge point
U_o	the velocity of jet at port

	the velocity of plume at port
U_c	the centerline velocity of jet
	the velocity at a distance r from the centerline of jet
	the time-averaged jet velocity distribution at a coordinate transverse r to the jet axis
\bar{U}	the jet centerline velocity at a distance z from port
	the plume centerline velocity at a distance z from port
V	the diffusion velocity in the y direction
V_f	the free stream velocity in full pipe
V_d	a densimetric velocity
W	the velocity of diffusion at z direction
Y	the rate of supply of tracer mass to a jet
Y_n	the depth of nozzle below sea water surface
	the depth of discharge below surface
a	the total cross-sectional area of ports on a single riser
b	the radius of jet
	the radius of plume
	the half width of jet
b_w	the value of r at which U_r reduces to some specified fraction of U_m
$b(x)$	the radius of a plume
b_1	an empirical constant
b_2	an empirical constant

c	the concentration of jet at a point r from axis and a distance x from outlet
c_m	the concentration of jet on axis at distance x from outlet
c_0	the initial concentration of jet
c_1	an empirical constant
c_2	an empirical constant
d	the jet diameter
d_p	the diameter of jet at port the diameter of plume at port
$erf \{ \}$	an error function $\{ \}$
f	a Gaussian function a tunnel friction factor
g	gravitational acceleration
h	the height of riser port above tunnel centerline
k	a dimensionless coefficient a bacterial decay coefficient
l_Q	a characteristic length scale for a jet
l_M	a characteristic length scale for a buoyant jet
q	a vector of mass flux with components (q_x, q_y, q_z) in a Cartesian coordinate system
r	the ratio of circulating flow to the sewage flow the radial distance measured from the centerline of jet
s	the axial distance of plane from nozzle

t	a contact time
u	a vertical velocity the velocity of jet at a point r from axis and a distance x from outlet
$u(x, \tau)$	a vertical velocity
u_a	the ambient current velocity
u_j	a jet velocity
u_m	the velocity of jet on axis at distance x from outlet
u_o	the initial velocity of jet at port
w	the time-averaged jet velocity
w_m	the time-averaged vertical velocity on the axis of the plume
x	the distance of the die-off or disappearance of coliform bacteria
z	the distance of jet from port the distance of plume from port the cartesian coordinate direction distance along the jet axis
Δ	the buoyancy force of plume at port
$\Delta\rho$	the difference densities between the receiving fluid and the fluid in jet the density difference between seawater and effluent
$\Delta\rho_o$	the initial difference density of jet
$\bar{\Delta}$	the buoyancy force of plume at a distance z from port
α	the constant relating inflow velocity at the edge of the plume to the vertical velocity inside the plume the dimensionless constant of proportionality

	a diffusivity constant
α_w	an entrainment coefficient depending primarily on wave condition
α_w	a coefficient depending on the wave and jet velocity
β	an angle that the jet axis makes with the horizontal axis at any distance 's' along jet axis
ϵ_0	the initial value of horizontal turbulent diffusion coefficient
ϵ_x	the turbulent diffusion coefficient in x direction
ϵ_y	the turbulent diffusion coefficient in y direction
ϵ_z	the turbulent diffusion coefficient in z direction
θ	a pipe inclination
	a tunnel slope
λ	a dimensionless spread ratio
μ	a dimensionless coefficient
ρ	the density of plume
ρ_a	the density of ambient flow
	the density of fluid outside plume
ρ_j	the density of jet discharge
	the initial density of plume
	the density of seawater
ρ_e	the density of effluent
$\rho(x,t)$	the density of plume
ρ_f	the density of freshwater

	the density of fluid being discharged
ρ_s	the density of seawater
	the density of receiving fluid
ν	a kinematic viscosity
ν	the viscosity of fluid
ψ	the friction of riser

Chapter 1

Introduction

1.1. Sea outfalls for delivery of effluents to ocean

Sea outfalls are constructed to deliver effluents from land-based treatment or domestic/industrial areas directly to the ocean. The effluents mix with ambient sea water near the outlet point (initial dilution) and rise to the ocean surface. Besides that, the effluents spread away from the discharge point and experience secondary dilution. The effectiveness of the sea outfall primarily depends on the degree of the initial effluent dilution between the outfall diffuser and the ocean surface.

The simplest sea outfall consists of a long pipe with a circular nozzle at the end of the pipe. This may be used for very small discharges. For large discharges, the effluent flows through a sea outfall which has a multipoint diffuser attached to increase the initial dilution. The multipoint diffuser consists of a series of ports located along the pipe (Figure 1.1).

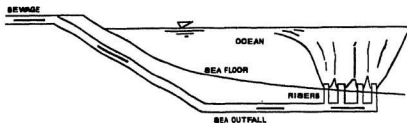


Figure 1.1. Schematic diagram of sea outfall

Due to increasing effluent discharges from large cities, the need to minimize maintenance along the foreshore, and improvements in tunnel technology, effluents may also be discharged through a tunnel and released into the ocean through a series of vertical shafts or risers. At the head of the risers are attached diffusers to minimize the initial dilution. The tunnel outfall is better suited to large discharges than a pipe outfall. An example is the Boston Wastewater Outfall at Boston, USA.

The Boston wastewater outfall is designed to discharge effluents (from a peak design flow of $56 \text{ m}^3/\text{s}$ to a minimum of $14 \text{ m}^3/\text{s}$) from Massachusetts Water Resources Authority (MWRA)'s Secondary Treatment Plant on Deer Island into Massachusetts Bay. This outfall has an internal diameter of 7.3 m and a length of 14,000 m to the diffuser zone with a 1:2,000 upward slope. It terminates in a 2,000 m diffuser consisting of 80 risers, 76 cm in diameter, each with eight radial ports with conical nozzles attached. The port diameter is 13 cm. The risers are about 76 m long from the tunnel to the seabed ("Secondary" 1988). Based on a study of dilution, the number of risers was

changed from 80 to 55 (Roberts, 1993).

For many years, sea outfalls have not acted according to their design expectation. Bennet (1981), Munro D. (1981), and Charlton (1982a) have all indicated that a reduction of the effluent discharge through the diffuser permits the intrusion of seawater into the outfall. To solve this problem, many studies have been done in the laboratory to determine the process of saline intrusion (Charlton 1982b, Davis, *et al.* 1988, and Wilkinson 1985) and to find how to purge the saline intrusion from the outfall (Wilkinson 1984, Charlton, *et al.* 1987, Burrows, *et al.* 1991, and Wilkinson and Nittim 1992, Adams, *et al.* 1994). Charlton (1985a) has described a variety of ways to prevent sea water intrusion.

1.2. Sea outfalls for Indonesia

Indonesia consists of many islands and most of the capital cities of the province are located near the sea (see Figure 1.2). The growth of cities correlates to an increase in the disposal of industrial and/or domestic effluents which need a simple treatment process to purify the effluents. The limitation and the high costs of the land area, together with the high costs of conventional land based treatment building and maintenance, suggests that the government should perhaps choose an alternative treatment.

The sea outfall is a most appropriate choice. The land area requirement of a sea outfall is relatively small. It requires less capital expenditure in construction, less cost in

maintenance, and less operator attention (Sharp, 1990). Besides that it has a lower capital cost and causes less damage to the environment (Allen and Sharp, 1987). Especially for Indonesia as a developing country, the limitation on the availability of highly skilled labour and financial resources indicates the choice of a waste water treatment which requires low technology, low cost, and intensive labour.

1.3. Objective of this study

The primary objective of this study was to investigate some different ways of reducing the magnitude of the flow needed to purge a sea outfall. Saline wedge profiles, condition of flow in the risers, and purging discharges, are compared for a variety of conditions. These included studies of risers with and without caps (one port and two ports with each diameter 2.54 cm (one inch)), studies of jets located under the risers and located upstream of the risers, air bubbles discharged under the risers, and a barrier constructed across the top of the tunnel and located upstream of the risers. The study was experimentally oriented in which saline wedge profiles were measured at different discharges in order to determine the effect of the various changes made to the system.

Chapter 2

Literature Review

2.1. Jet, plume, and buoyant jet

2.1.1. General

Different terms are used to describe the discharge of a fluid through an orifice or a circular nozzle into a large body of the same or different fluid. The use of different terms depends on momentum and buoyancy effects. Given the same density between the two fluids, the momentum effects become very important and this is termed a jet. The trajectory of the jet is a straight line. A plume is the term for flow that results from an initial difference in density but with no initial momentum. The flow is then influenced only by buoyancy effects. If there are differences in densities and initial momentum is also present in the flow, the flow is called a buoyant jet.

2.1.2. Jet

A jet occurs when a fluid is discharged into a large body of fluid with the same density, such as a freshwater effluent discharged into a freshwater lake. The trajectory of the flow is a straight line and the jet mixes strongly with the surrounding fluid creating turbulence, causing the jet to grow thicker.

Albertson, *et al.* (1950) proposed the flow pattern shown in Figure 2.1. This figure shows the zone of establishment and the zone of established flow. The zone of flow establishment (ZFE) is the region less than six times the diameter of the jet. In this region, the centerline velocity is constant and is the same as the velocity at the nozzle U_o . The region more than six jet diameters downstream is termed the zone of established

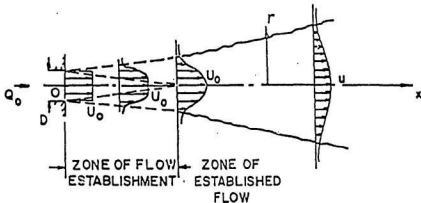


Figure 2.1. Zone of flow establishment (ZFE) and zone of established flow (ZEF)(Albertson *et al.*, 1950)

flow (ZEF). The time-averaged jet velocity distribution U , at a coordinate transverse r to the jet axis can be written by a function in the form

$$U_r = U_m f\left(\frac{r}{b_m}\right) \quad (2.1)$$

where

U_m = velocity of jet centerline

b_m = value of r at which U_r reduces to some specified fraction of U_m [0.5 or 0.37 ($= e^{-1}$)]

f = a Gaussian function.

Fischer *et al.* (1979) analyzed velocity and concentration on the axis of the jet by using the concepts of characteristic length. The characteristic length scale for the jet l_Q in terms of the initial volume flux Q and momentum flux M is given by the following equation:

$$l_Q = \frac{Q}{M^{1/2}} = \sqrt{A} \quad (2.2)$$

where

Q = initial volume flux of jet = $w\pi d^2/4$

M = initial specific momentum flux of jet = $w^2\pi d^2/4$

d = diameter of jet

w = time-averaged jet velocity

A = initial cross sectional area of jet

The characteristic length scale for a round jet with diameter d , $l_Q = \sqrt{\pi/4} d$ and for a planar jet is the slot width.

The centerline velocity and the centerline tracer concentration of jet can be estimated by using the following equation (Wood, *et al.* 1993):

$$\frac{\bar{U}}{U_o} = K_{ju} \left(\frac{\pi}{4} \right)^{0.5} \left(\frac{z}{d_p} \right)^{-1} \quad (2.3)$$

and

$$\frac{\bar{C}}{C_o} = K_{jc} \left(\frac{4}{\pi} \right)^{0.5} \left(\frac{z}{d_p} \right)^{-1} \quad (2.4)$$

and

$$\frac{b}{z} = K_{jb} \quad (2.5)$$

where

\bar{U} = centerline velocity of jet at a distance z from port

U_o = port velocity of jet

\bar{C} = centerline concentration of jet at a distance z from port

C_o = port concentration of jet

z = distance of jet from port

b = radius of jet

d_p = port diameter of jet

K_m, K_b, K_z = coefficient that can be determined experimentally as 7.57, 0.11 and 6.06 (Papanicolaou, 1984)

The inverse of the equation (2.4) is the centerline dilution ($S = C_c/\bar{C}$).

2.1.3. Plume

When a fluid is discharged into another fluid through an orifice with a density difference but without initial momentum, it is termed a buoyant plume. Fischer *et al.* (1979) analyzed the velocity on the plume axis. The time-averaged vertical velocity on the axis of the plume w_m must be a function of the buoyancy flux B , the distance from the orifice z , and the viscosity of the fluid ν . This is illustrated in the following equation:

$$w_m = f(B, z, \nu) \quad (2.6)$$

where

B = initial specific buoyancy flux = $Q(\Delta\rho/\rho_1)g$

$\Delta\rho$ = difference densities between the receiving fluid and the fluid in jet = $\rho_2 - \rho_1$

ρ_1 = density of fluid being discharged

ρ_2 = density of receiving fluid

g = gravitational acceleration

Q = initial volume flux of jet

z = cartesian coordinate direction distance along jet axis

ν = viscosity of fluid.

According to dimensional analysis with four variables, there are two dimensionless groups as:

$$w_m \left(\frac{z}{B} \right)^{1/3} = f \left(\frac{B^{1/3} z^{2/3}}{\nu} \right) \quad (2.7)$$

The right term is a form of Reynolds number. If $z \gg \nu^{3/2}/B^{1/2}$, the flow is fully turbulent and there is no effect of viscosity, hence the left term is constant and Equation (2.7) becomes:

$$w_m = b_1 \left(\frac{B}{z} \right)^{1/3} \quad (2.8)$$

Rouse *et al.* (1952) found that $b_1 = 4.7$.

The time-averaged maximum tracer concentration C_m can be estimated by using the following equation:

$$\left(\frac{C_m}{Y} \right) = \left(\frac{b_4}{B^{1/3} z^{2/3}} \right) \quad (2.9)$$

where

b_4 = empirical constant = 9.1 (Chen and Rodi, 1976)

Y = rate of supply of tracer mass to a jet

The centerline velocity and the buoyancy force of the plume can be estimated by using the following equation (Wood, et al. 1993):

$$\frac{\bar{U}}{U_o} = K_{pU} \left(\frac{\pi}{4} \right)^{0.33} Fr_o^{-0.66} \left(\frac{z}{d_p} \right)^{-0.33} \quad (2.10)$$

and

$$\frac{\bar{\Delta}}{\Delta_o} = K_{p\Delta} \left(\frac{\pi}{4} \right)^{0.66} Fr_o^{0.66} \left(\frac{z}{d_p} \right)^{-1.66} \quad (2.11)$$

and

$$\frac{b}{z} = K_{pb} \quad (2.12)$$

where

\bar{U} = centerline velocity of plume at a distance z from port

U_o = port velocity of plume

$\bar{\Delta}$ = buoyancy force of plume at a distance z from port

Δ_o = buoyancy force of plume at port

Fr_o = densimetric Froude number at origin ($U_o / (\Delta_o d_p)^{0.5}$)

z = distance of plume from port

b = radius of plume

d_p = port diameter of plume

K_{pU} , K_{pb} , $K_{p\Delta}$ = coefficient of plume that can be determined experimentally as 3.85, 0.105 and 11.1 (Papanicolaou, 1984).

The inverse of the equation (2.11) is the centerline dilution ($S = \Delta_o / \bar{\Delta}$).

2.1.4. Buoyant Jet

A buoyant jet is a jet whose density initially differs from the density of the receiving seawater. The effluent flows through a submerged sea outfall into the receiving seawater and is influenced by the initial momentum and buoyancy effects. The mixed effluent may reach a density equal to that of the receiving seawater at some intermediate depth.

2.1.4.1. Horizontal buoyant jet

Abraham (1963, 1965) studied the buoyant jet phenomena by assuming that the distribution of velocity of a buoyant jet was gaussian (Figure 2.2). The distribution of velocity and tracer concentration at any cross section of the jet were presented as:

$$\frac{U_m}{U_r} = e^{-k(r/r_0)^2} \quad (2.13)$$

and

$$\frac{C_m}{C_r} = e^{-\mu k(r/r_0)^2} \quad (2.14)$$

where

U_m = centerline velocity of jet

U_r = velocity at a distance r from centerline of jet

C_m = centerline concentration of jet

C_r = concentration at a distance r from centerline of jet

r = radial distance measured from centerline of jet

s = axial distance of plane from nozzle

k = dimensionless coefficient = $-304(\beta/\pi)^3 + 228(\beta/\pi)^2 + 77$

μ = dimensionless coefficient = $0.96(\beta/\pi)^3 - 0.72(\beta/\pi)^2 + 0.80$

β = angle that jet axis makes with horizontal axis at any distance 's' along jet axis.

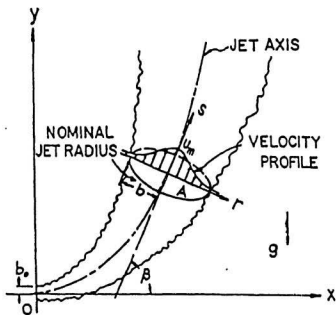


Figure 2.2. Cross sectional profile of a buoyant jet (Abraham, 1963)

Fan and Brooks (1966) proposed a similar solution by assuming that the rate of entrainment was related to the local characteristic velocity U_m and the local characteristic radius of the jet or plume b . This approach was used by Morton *et al.* (1956) and led to the following equation:

$$\frac{dQ}{ds} = \frac{d}{ds}(\pi U_m b^2) = 2\pi\alpha b U_m \quad (2.15)$$

where α is a dimensionless constant of proportionality.

The velocity and concentration distribution were shown in a slightly different form from that of Abraham's equations (Equations 2.13 and 2.14) as:

$$\frac{U_m}{U_r} = e^{-(\eta/b)^2} \quad (2.16)$$

and

$$\frac{C_m}{C_r} = e^{-(\eta/\lambda b)^2} \quad (2.17)$$

where

λ = dimensionless spread ratio

b = half width of jet.

The rate of volume flux (Equation 2.15) formed the basis for developing four ordinary differential equations, namely Continuity, Momentum, Buoyancy flux and the geometry of the jet. The main advantage of the entrainment equation over Abraham's

approach is that it is flexible and can be used for a variety of problems involving buoyant jets and plumes in a stratified environment. The plume width and distance 's' are not required to be specified in advance but can be derived from equations of motion and continuity.

Fischer *et al.*(1979) used dimensional analysis to determine the velocity on the centerline of the jet. The basic variables involved in a vertical buoyant jet within stagnant receiving water can be expressed as:

$$\phi(Q, M, B, z) = 0 \quad (2.18)$$

where

$$Q = \text{initial volume flux of jet} = w\pi d^2/4, [L^3/T]$$

$$M = \text{initial specific momentum flux of jet} = w^2\pi d^3/4, [L^4/T^2]$$

$$B = \text{initial specific buoyancy flux of jet} = g(\Delta\rho/\rho_0)Q, [L^4/T^3]$$

$$z = \text{cartesian coordinate direction distance along jet axis, [L].}$$

The non dimensional equation can be obtained as:

$$\phi\left(\frac{M^{1/2}z}{Q}, \frac{B^{1/2}z}{M^{3/4}}\right) = 0 \quad (2.19)$$

The first parameter of Equation (2.19) shows the initial momentum and volume flux which is important in the jet analysis. The second parameter is influenced by the

initial buoyancy and momentum. Any flow variable can be written as a function of these two variables, ie.

$$w = \frac{Q}{M} = f \left[\frac{M^{1/2} z}{Q}, \frac{B^{1/2} z}{M^{3/4}} \right] \quad (2.20)$$

Following the limiting conditions where flow has initial momentum M and initial buoyancy B , but no initial volume flux Q , the solution of w_m for a round jet can be obtained from the following equation:

$$w = \frac{M^{1/4}}{B^{1/2}} = f \left(\frac{B^{1/2} z}{M^{3/4}} \right) \quad (2.21)$$

By developing equation (2.21), Fisher *et al.* (1979) derived the following equation:

$$w = \frac{M^{1/4}}{B^{1/2}} = c_1 \left(\frac{M^{3/4}}{B^{1/2} z} \right), \text{ for } z < \frac{M^{3/4}}{B^{1/2}} \quad (2.22)$$

and

$$w = \frac{M^{1/4}}{B^{1/2}} = c_2 \left(\frac{M^{3/4}}{B^{1/2} z} \right)^{1/3}, \text{ for } z > \frac{M^{3/4}}{B^{1/2}} \quad (2.23)$$

where c_1 and c_2 are empirical constants.

If the buoyant jet is jetlike or plume-like, it is possible to compute the ratio of z to l_M , where $l_M = M^{3/4}/B^{1/2}$. For $z \gg l_M$, the flow is like a plume and for $z \ll l_M$ the flow is like a jet. Comparing z and $l_Q = Q/M^{1/2}$, if $z \gg l_Q$, the flow is a fully developed jet and if $z \sim 0$ then the flow is still controlled by the jet exit geometry. The ratio of l_Q to l_M is termed the jet Richardson number R_j :

$$R_j = \frac{l_Q}{l_M} \quad (2.24)$$

2.1.4.2. Vertical buoyant jet

Morton, Taylor and Turner (Morton *et al.*, 1956) studied buoyant plumes by assuming that the entrainment at any cross section is related to some basic characteristic velocity at that section, that the profiles of velocity and buoyancy across the plume are similar at different heights, and that the variations of local density are small relative to the density of the ambient fluid at the source.

Morton *et al.* (1956) defined the flow parameters used to analyze the buoyant plume as shown in Figure 2.3. Assuming that velocity and buoyancy force across the plume are constant, three equations were derived. The equations are given below:

- By using the principle of volume conservation

$$\frac{d}{dx}(\pi b^2 u) = 2\pi b \alpha u \quad (2.25)$$

- By using the principle of mass conservation

$$\frac{d}{dx}(\pi b^2 u^2 \rho) = \pi b^2 g(\rho_a - \rho) \quad (2.26)$$

- By using the principle of density difference conservation

$$\frac{d}{dx}(\pi b^2 u(\rho_o - \rho)) = 2\pi b \alpha u(\rho_o - \rho) \quad (2.27)$$

where

b = radius of plume

u = velocity in vertical direction,

ρ = density of plume

ρ_a = density of ambient fluid outside plume

ρ_o = initial density of plume

α = constant relating to inflow velocity at edge of plume to vertical velocity inside plume.

Rearranging the above equations, the equations of velocity and concentration along the axis of the jet can be derived as:

$$u = \frac{5}{6\alpha} \left(\frac{9}{10} \alpha Q \right)^{1/3} x^{-1/3} \quad (2.28)$$

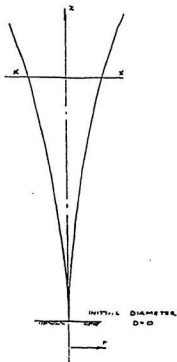
and

$$g \frac{(\rho_o - \rho)}{\rho} = \frac{5Q}{6\alpha} \left(\frac{9}{10} \alpha Q \right)^{1/3} x^{-9/3} \quad (2.29)$$

where

Q = initial discharge of jet

g = gravitational acceleration



At section $x-x$:

$u(x,r) = u$ = vertical velocity

$b(x) = b$ = radius of plume

$\rho(x,r) = \rho$ = density of plume

ρ_o = density of ambient fluid outside plume

ρ_o = initial density of plume

α = constant relating vertical velocity inside plume

Figure 2.3. Parameters of flow involved in theoretical analysis of buoyant plume (Morton et al., 1956)

Comparing the above solution with experimental results and also the results given by Schmidt (1941) and Rouse *et al.* (1952) gave the value of $\alpha = 0.093$ and the gaussian profile of vertical velocity and concentration as

$$u = u_m \exp\left[-8\alpha\left(\frac{r}{x}\right)^2\right] \quad (2.30)$$

and

$$c = c_m \exp\left[-8\alpha\left(\frac{r}{x}\right)^2\right] \quad (2.31)$$

where

u = velocity of jet at a point r from axis and a distance x from outlet

c = concentration of jet at a point r from axis and a distance x from outlet

u_m = velocity of jet on axis at distance x from outlet

c_m = concentration of jet on axis at distance x from outlet

$$= (\rho_s \cdot \rho) / (\rho_s \cdot \rho_0)$$

Abraham (1963) analyzed the diffusion of a jet in a liquid which had a greater density and suggested that the factor x in the above equations for a finite initial diameter d and velocity u_0 should be changed to be $(x+2d)$. He defined the value of Q as

$$Q = \frac{\pi d^2 u_0 (\rho_s - \rho_0)}{4 \rho_0} \quad (2.32)$$

The densimetric Froude number F_Δ is given by

$$F_\Delta = \frac{Q}{\frac{\pi d^2}{4} \left(\frac{\rho_a - \rho_o}{\rho_o d} \right)^{1/2}} \quad (2.33)$$

Equation (2.30) and (2.31) were then modified as:

$$\frac{u_m}{u_o} = 3.65 F_\Delta^{-2/3} \left(\frac{x}{d+2} \right)^{-1/3} \exp \left[-80 \left(\frac{r}{x} \right)^2 \right] \quad (2.34)$$

and

$$\frac{c_m}{c_o} = 9.7 F_\Delta^{-2/3} \left(\frac{x}{d+2} \right)^{-5/3} \exp \left[-80 \left(\frac{r}{x} \right)^2 \right] \quad (2.35)$$

where

u_o = initial velocity of jet

c_o = initial concentration of jet

2.2. Dilution

Wastewater effluent flows through a sea outfall into the sea in two different phases namely initial buoyant rise and secondary buoyant spreading at the surface. Initial dilution occurs as the effluent combines with the seawater near the outlet point or nozzle of the jet. Secondary dilution occurs as the effluent moves away from the mixing zone and then mixes with the seawater at some intermediate depth or at the sea surface.

2.2.1. Initial dilution

The first experiments on buoyant jets were carried out by Rawn and Palmer (1930) who investigated buoyant jets in Los Angeles harbour. Dye samples were taken at the boil of the jet and the dilution was measured. Empirical formula were obtained from these experiments which later proved to be not particularly useful. Rawn, Bowerman and Brooks (1960) reanalysed the Rawn and Palmer data to estimate the densimetric Froude number F_d , the Reynolds number R_e , and the relative depth Y_e/d . They developed the following equation by using partial analysis:

$$S_o = \phi \left(F_d, R_e, \frac{Y_e}{d} \right) \quad (2.36)$$

where

S_o = dilution of jet fluid defined as ratio of jet fluid concentration at any point to jet fluid concentration at discharge point

F_d = densimetric Froude number

R_e = Reynolds number

Y_e = depth of nozzle below seawater surface

d = initial diameter of jet

Rawn, Bowerman and Brooks (1960) found that the Reynolds number had no significant effect when it was greater than 5000. This suggests that the flow is fully turbulent and has no appreciable effect on the initial dilution S_o . Hence, Equation (2.36) was modified to:

$$S_o = \phi\left(F_A, \frac{Y_o}{d}\right) \quad (2.37)$$

The initial dilution by Rawn, Bowerman and Brooks (1960) is shown in Figure 2.4.

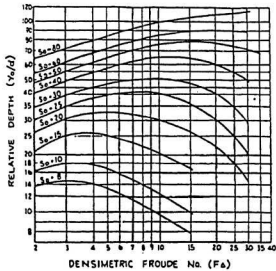


Figure 2.4. Initial dilution after Rawn, Bowerman and Brooks (1960)

Cederwall (1963) measured the dilution at the centerline of the jet from the mixing of salt water and freshwater. He found that maximum concentrations occur along the axis of the jet. According to this conclusion, Rawn *et al.* (1960) showed that the dilution at large densimetric Froude number predicted was greater than the measured minimum dilution at centerline.

Frankel and Cumming (1965) conducted some experiments and found that the concentration distribution across the jet was approximately Gaussian, that the horizontal jet was the most efficient, and that the vertical jet was least efficient. They concluded that the effective depth to diameter ratio is less than the available surface depth to diameter ratio which suggests that the centerline dilution of the plume can be estimated solely as a function of the depth of nozzle below the surface. The effective mixing depth was found to be two thirds of the available depth.

Sharp (1968) discussed Abraham's predicted dilutions and those of Rawn and Palmer (1930) and noted that the values of dilution at lower densimetric Froude number were similar, but at the large values, Abraham's dilutions were lower than Rawn and Palmer's. He concluded that this might have been due to still water conditions for Abraham whereas these may have been some turbulence in the field study of Rawn and Palmer. The approach followed by Rawn and Palmer was difficult because it was not easy to take samples at the point where minimum dilution was located.

Cederwall (1968) estimated the initial dilution for a horizontal buoyant jet and developed an empirical formula:

$$S_o = 0.54F_{\Delta} \left[\frac{(Y/d)}{F_{\Delta}} \right]^{0.716} \quad \text{for } \frac{Y/d}{F_{\Delta}} < 0.5 \quad (2.38)$$

and

$$S_o = 0.54F_{\Delta} \left[0.38 \frac{(Y/d)}{F_{\Delta}} + 0.66 \right]^{0.93} \quad \text{for } \frac{Y/d}{F_{\Delta}} > 0.5 \quad (2.39)$$

Liseth (1970) developed a generalised chart by combining the results of various workers. The chart can be seen in Figure 2.5. He concluded that surface dilutions estimated by theoretical solutions were higher than experimental results.

• Effect of currents

Currents can cause the increase of dilution in the receiving seawater. Agg and Wakeford (1972) developed an equation for minimum centerline dilution using linear regression of the data collected at five marine outfalls around the coast of England. They assumed the distribution of the average dilutions to be Gaussian (average dilution = 1.7 x minimum dilution). The resulting equation was given as:

$$\frac{S_m}{S_o} = 7.526 \left(\frac{U_c}{U_o} \right)^{0.938} \quad (2.40)$$

where

S_m = minimum centerline dilution at surface

S_o = still water dilution under identical conditions of depth and density difference

U_a = velocity of ambient current

U_j = velocity of jet at outfall

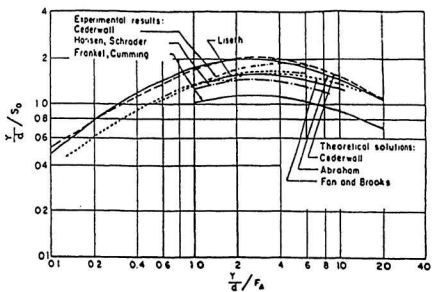


Figure 2.5. Generalised chart of various workers for surface dilution of a buoyant jet (Lieth, 1970)

Bennett (1981, 1983) developed an empirical equation for the ratio of moving water to still water dilution and used Cederwall's equation. He obtained a correction factor ($CF = S_m/S_o$) in terms of ambient current velocity U_a , jet velocity U_j , and depth below surface Y_s :

$$\log_{10} CF = 1.554 + 0.684 \log_{10} U_a - 0.467 \log_{10} U_o - 0.297 \log_{10} Y_o \quad (2.41)$$

He also obtained the measured moving water dilution using linear regression directly as a function of U_a , Y_o , and U_o or discharge Q . This gave the following equation:

$$S_m = 55.59 \left(\frac{U_a^{0.682}}{U_o^{0.925}} \right) Y_o^{1.183} \quad (2.42)$$

Bennet recommended this equation to be suitable for practical design purposes.

Sharp and Moore (1987) also developed a new equation using the complete data base, comprising both sets of data, namely Agg and Wakeford's and Bennett's. The equation is

$$S_m = S_o + 1.57 \left(\frac{U_a}{U_o} \right)^{0.359} S_o^{1.33} \quad (2.43)$$

where

S_m = moving water dilution

S_o = still water dilution

U_a = current velocity

U_o = velocity of jet

Y_o = depth of receiving water below the surface

Lee and Neville-Jones (1987) predicted the initial dilution of buoyant sewage discharge in moving water by assuming that the buoyant sewage discharge is a source of mass (volume), momentum, and buoyancy. The following equations are given for the buoyancy dominated near field (BDNF) and far field (BDFF) as

BDNF :

$$S_m = C_1 \frac{B^{1/3} H^{2/3}}{Q} \quad \text{for } \frac{HU_a^3}{B} < 5 \quad (2.44)$$

and

BDFF :

$$S_m = C_2 \frac{U_a H^2}{Q} \quad \text{for } \frac{HU_a^3}{B} \geq 5 \quad (2.45)$$

where

S_m = minimum surface dilution

C_1 = dilution constants for BDNF

C_2 = dilution constant for BDFF

H = depth of jet discharge below surface

U_a = velocity of ambient current

Q = volume flux of jet discharge = $U_j \pi d^2 / 4$

U_j = velocity of jet

d = diameter of jet

B = discharge specific buoyancy flux = $Q(\Delta\rho/\rho_a)g$

$\Delta\rho$ = initial density difference = $(\rho_a - \rho_j)$

ρ_a = density of jet discharge

ρ_j = density of ambient flow

The value of $C_1 = 0.31$ and $C_2 = 0.32$ for the mean value of the minimum initial dilution.

Lee and Cheung (1991) showed that jet behaviour for the discharges which are dominated by buoyancy is governed by the dimensionless depth HU_a^3/B , where H is the depth of the jet discharge below the surface, B is the discharge buoyancy flux and U_a is the velocity of ambient current. Both the width of jet and dilution increase substantially even in weak current.

- Effect of waves

Beside the current of seawater, waves also may cause the increase of dilution. The effect of waves depend on the type of the wave.

Shuto and Ti (1974) developed empirical equations based on their experiments with small jets discharged under standing waves in a 0.5 m wide wave channel. The surface dilution (S_s) can be estimated by the following equation:

$$S_w = 1.27 \left(\frac{\alpha_w^2}{F_d} \right) \left(\frac{H_w}{d} \right) \left(\frac{Y_e}{d} \right)^{3/2} \quad (2.46)$$

where

F_d = densimetric Froude number = $U_e/(gd)^{1/2}$

H_w = wave height

d = diameter of jet

Y_e = depth of discharge

U_e = velocity of jet

g = gravitational acceleration

α_w = entrainment coefficient depend primarily on wave condition

The centerline dilution at the point measurement, x , can be calculated by the following equation as a linear function of the horizontal co-ordinate, x :

$$S_w = 1.15 \left(1 + 2.24 \alpha_w \frac{x}{d} \right) \quad (2.47)$$

where α_w is a coefficient depends on the wave and jet velocities.

Sharp (1986) did qualitative experiments and indicated that the jet structure under shallow waves was different from deep waves. The jet under shallow water waves broke into two distinct clouds of effluent. Jets in deep water waves were not significantly different from those in still water. So, a single theory cannot be used for all wave types.

According to Fischer's work (Fischer *et al.*, 1979), Chin (1987) identified the relevant length scales and got the following equation:

$$\frac{S_w}{S} = 1 + 6.15 \left(\frac{U_{max}}{U_o} \right) \quad (2.48)$$

where

S_w = average surface dilution with waves

S = average surface dilution without waves

U_o = velocity of jet

U_{max} = maximum horizontal wave-induced velocity at discharge point

$$= (gT_w(H_w/L_w)) / (2 \text{Cosh}(2\pi Y_o/L_w))$$

g = gravitational acceleration

T_w = wave period

H_w = wave height

L_w = wave length

Y_o = depth of discharge below surface

2.2.2. Secondary dilution

Following discharge at depth, the effluent mixes with the receiving seawater and rises to the sea surface or to a position of vertical stability below the surface. The mixture of effluent and seawater then moves horizontally due to local current systems and spreads due to buoyant and diffusive mechanisms. The secondary dilution involves both an advective component (which is the process of transport) and a diffusive component (which is the process of mixing)

in distribution process.

Adolph Fick (1855), a German physiologist, proposed a law popularly known as Fick's law. This law states that the solute mass flux, q , which is the mass of solute crossing a unit area per unit time in a given direction, correlates with the gradient of solute concentration directly. This can be written in a one-dimensional diffusion process as:

$$q = -D \frac{\partial C}{\partial x} \quad (2.49)$$

where

D = coefficient of proportionality or diffusion coefficient

C = diffusing solute concentration mass

$(-)$ = solute mass flux move from high to low concentrations

In three dimensions, Fick's law can be expressed as:

$$q = -D \nabla C \quad (2.50)$$

where q is the vector of mass flux with components (q_x, q_y, q_z) in a Cartesian coordinate system.

The equation for conservation of mass in one dimension is

$$\frac{\partial q}{\partial x} + \frac{\partial C}{\partial t} = 0 \quad (2.51)$$

The relationship of the flux $q(x,t)$ and concentration $C(x,t)$ is shown in the equation (2.51).

The spreading of mass in a fluid with no velocity in Cartesian coordinates is defined by the following equation:

$$\frac{\partial C}{\partial t} = D \left(\frac{\partial^2 C}{\partial x^2} + \frac{\partial^2 C}{\partial y^2} + \frac{\partial^2 C}{\partial z^2} \right) \quad (2.52)$$

The total rate of mass transport is the advective plus diffusive flux:

$$q = UC + \left(-D \frac{\partial C}{\partial x} \right) \quad (2.53)$$

Equation (2.53) can be substituted in equation (2.51), to yield

$$\frac{\partial C}{\partial t} + \frac{\partial}{\partial x}(UC) = D \frac{\partial^2 C}{\partial x^2} \quad (2.54)$$

The equation of advective diffusion in Cartesian coordinates can then be written as

$$\frac{\partial C}{\partial t} + U \frac{\partial C}{\partial x} + V \frac{\partial C}{\partial y} + W \frac{\partial C}{\partial z} = D \left(\frac{\partial^2 C}{\partial x^2} + \frac{\partial^2 C}{\partial y^2} + \frac{\partial^2 C}{\partial z^2} \right) \quad (2.55)$$

where

U = velocity at x direction

V = velocity at y direction

W = velocity at z direction

This equation is simply called the "advective diffusion equation" due to the common feature of environmental problems for advection.

The advective diffusion equation can be simplified by assuming that there is only a mean velocity U in the x direction and that the diffusion coefficient D is the same in all directions. So, the diffusion equation can be written as

$$\frac{\partial C}{\partial t} + U \frac{\partial C}{\partial x} = D \left(\frac{\partial^2 C}{\partial x^2} + \frac{\partial^2 C}{\partial y^2} + \frac{\partial^2 C}{\partial z^2} \right) \quad (2.56)$$

By analogy, the equation of diffusion in a three-dimensional system in turbulent flow is given as:

$$\frac{\partial C}{\partial t} = \epsilon_x \frac{\partial^2 C}{\partial x^2} + \epsilon_y \frac{\partial^2 C}{\partial y^2} + \epsilon_z \frac{\partial^2 C}{\partial z^2} \quad (2.57)$$

where

C = mass concentration of diffusing solute

ϵ_x , ϵ_y , and ϵ_z = turbulent diffusion coefficients in x , y , and z directions.

In practical problems, the diffusion equation due to inhomogeneous turbulence can be written with spatially variable coefficients in the form

$$\frac{\partial C}{\partial t} + U \frac{\partial C}{\partial x} + V \frac{\partial C}{\partial y} + W \frac{\partial C}{\partial z} = \frac{\partial}{\partial x} \left(\epsilon_x \frac{\partial C}{\partial x} \right) + \frac{\partial}{\partial y} \left(\epsilon_y \frac{\partial C}{\partial y} \right) + \frac{\partial}{\partial z} \left(\epsilon_z \frac{\partial C}{\partial z} \right) \quad (2.58)$$

This equation is for moving and spreading.

Richardson's law (Richardson, 1926) states that the diffusion coefficient increases proportionally to the four-thirds power of the length of the patch of the solution. In the case of diffusing sewage, this would be a measure of the size of the initial sewage field above the outfall.

$$\epsilon = \alpha L^{4/3} \quad (2.59)$$

where

L = length of patch

α = diffusivity constant

According to Koh and Brooks (1975), the value of α ranges from 1.5×10^4 to 5×10^3 ft^{2/3}/s (0.0015 to 0.049 cm^{2/3}/s). Pearson (1961) suggested $\alpha = 0.001$ ft^{2/3}/s (0.01 cm^{2/3}/s).

Brooks (1960) analyzed secondary dilution (S_d) in a uniform current with diffusion only in the longitudinal direction. His solution is given by

$$S_d = \frac{C_o}{C_{max}} = \left\{ \operatorname{erf} \left[\frac{3/2}{(1 + 8\epsilon_o t/w^2)^3 - 1} \right] \right\}^{-1/2} \quad (2.60)$$

where

C_o = waste concentration after establishment of waste field but before further diffusion

C_{max} = centerline concentration after travel time t

ϵ_o = initial value of horizontal turbulent diffusion coefficient corresponding to width w

$\operatorname{erf} \{ \} =$ error function $\{ \}$

The error function $erf\{ \}$ is defined by the equation

$$erf\{ X \} = \frac{2}{\sqrt{\pi}} \int_0^X e^{-t^2} dt \quad (2.61)$$

Munro and Mollowney (1974) proposed a numerical model based on an onshore wind-induced surface current. In this model, the dilution is greatly reduced by vertical mixing and the compensating subsurface counter-current. Brooks method can be used to estimate the concentration at a distance from the source by assuming that the current runs in a direction from the source to the point of interest.

2.2.3. Bacterial decay

Bacterial decay is the process of the decrease of the bacterial concentration simultaneously with secondary dilution. The rate of decay in a stagnant water body is given by the following equation:

$$\frac{dC}{dt} = -kC \quad (2.62)$$

where

C = mass concentration

t = contact time

k = bacterial decay coefficient

The decrease of bacterial concentration is shown by the following equation:

$$C_t = C_o 10^{-t/T_{90}} \quad (2.63)$$

where

C_t = remaining coliform concentration after time t

C_o = initial coliform concentration

T_{90} = time required for 90% reduction in coliform concentration

The dilution due to die-off or disappearance of coliform bacteria (S_p) can be estimated by the following equation:

$$S_p = 10^{t/T_{90}} = 10^{x/(UT_{90})} \quad (2.64)$$

where

T_{90} = time taken for 90% decay

$x = Ut$.

U = mean velocity

The die-off factor (T_{90}) is the time over which 90 % of the initial number of coliform bacteria is inactivated. The concentration of coliforms is reduced by a combination of several factors, such as, sedimentation, predation by other organisms, pH, temperature, osmotic shock due to rapid changes in salinity, initial number of organisms, degree of treatment of the effluent, presence of organic material and chemicals, the ultra-violet component of solar radiation, and turbidity of the receiving waters. The most important is the ultra-violet radiation.

Due to initial dilution (S_1), secondary dilution (S_2), and bacterial die-off (S_3), total concentration of remaining coliform after time t (C_t) can be estimated by the equation

$$C_t = \frac{C_o}{S_1 S_2 S_3} \quad (2.65)$$

2.3. Saline intrusion and purging in sea outfalls

2.3.1. Saline intrusion

The effectiveness of the sea outfalls depends on the degree of initial effluent dilution between the outfall port and the sea surface. Because there are two different fluid densities, the denser seawater can intrude into the outfall. The presence of seawater in the outfall can then reduce the overall efficiency of the sea outfall. Beside that, sediments may be drawn into the outfall system via the discharge ports. In the longterm, the seawater and sedimentation may damage the sea outfall system. Grace (1985) for example, suggested that saline intrusion and marine life cause blocked risers and diffusers. This can result in the breaking away of risers from the manifold.

Seawater can intrude into the outfall due to a shutdown of effluent flow to the sea outfall, a reduction of effluent flow to the point where seawater is able to enter the diffuser ports, and following construction of the sea outfall and prior to its commissioning (Wood *et al.* 1993).

Sharp and Wang (1974) studied intrusion into a circular pipe. They produced a formula based on early work by Keulegan (1966). Keulegan's work was done in an open channel and by changing the terms from an open channel system to a pipe flow system, the saline wedge length within a submerged open ended pipe could be estimated empirically. The formula is given as:

$$\frac{L_w}{D} = K \left[\frac{2V_r}{V_\Delta} \right]^{-3.4} \left[\frac{V_\Delta D}{\nu} \right]^{-0.76} \quad (2.66)$$

where

L_w = saline wedge length

D = diameter of pipe

K = numerical constant

V_r = free stream velocity in full pipe

ν = kinematic viscosity

V_Δ = densimetric velocity

The densimetric velocity (V_Δ) is given as:

$$V_\Delta = \left[gD \left(\frac{\rho_2 - \rho_1}{\rho_1} \right) \right]^{1/2} \quad (2.67)$$

where

D = diameter of pipe

g = gravitational acceleration

ρ_1 = density of freshwater

ρ_2 = density of seawater

Charlton (1985a) gave the value of K as approximately 12000 so that theoretical results would agree with experimental results.

Charlton (1985a) defined the scale of saline intrusion within an outfall as being either primary or secondary. Primary intrusion occurs when salt water penetrates the diffuser cap but is contained by a salt wedge and can be cleared by a small increase in discharge. This is not a serious hydraulic problem. Secondary intrusion occurs when the salt wedge passes through the diffuser cap and down the riser into the main outfall pipe. This causes a change in the hydraulic system and requires a large increase in discharge to remove the salt wedge. Secondary intrusion always occurs during the shut down periods of the outfall. It is acceptable if the design of the outfall is based on the initial peak flow rates, so that purging always occurs again after start up.

Charlton *et al.* (1987) mentioned that the seawater intrusion occurred through two phases (i.e. primary and secondary phases). Primary intrusion is the process of seawater intrusion when freshwater of density ρ_1 meets and flows over more dense seawater of density ρ_2 . This corresponds to the criterion that the densimetric Froude number (F_d) of the port is less than unity ($F_d < 1$). Secondary intrusion occurs when the discharge of freshwater reduces to a value where the wedge flow spills into a vertical riser section of the system.

The densimetric Froude number at a port (F_Δ) is given by

$$F_\Delta = \frac{U_o}{\sqrt{\Delta g d}} \quad (2.68)$$

where

U_o = port velocity of jet

$\Delta = (\rho_2 - \rho_1) / \rho_1$

ρ_1 = density of freshwater

ρ_2 = density of seawater

g = gravitational acceleration

d = port diameter

Davies, *et al.* (1988) undertook a series of experiments on primary intrusion and salt wedge formation in a smooth circular pipe. They found an empirical formula for a horizontal pipe ($\theta = 0$) in the form

$$\frac{L_o}{D} = K (2F_\Delta)^{-7.93} Re_\Delta^b \quad (2.69)$$

in which

$$K = 0.054(2F_\Delta)^{-3.669} \ln(2F_\Delta) \quad (2.70)$$

and

$$b = 0.56(2F_{\Delta})^{0.89} \quad (2.71)$$

where

L_w = arrested wedge length

D = diameter of pipe

F_{Δ} = densimetric Froude number

Re_{Δ} = densimetric Reynolds numbers.

They also found an empirical formula for an inclined pipe ($\theta \neq 0$). The equation is given as

$$\frac{L_w}{D} = K_2(2F_{\Delta})^p \quad (2.72)$$

in which

$$K_2 = (670.0)\theta^{0.71} \quad (2.73)$$

and

$$p = (137.0)\theta^{0.65} \quad (2.74)$$

where θ is the pipe inclination.

2.3.2. Purging

A sea outfall is usually flooded with seawater after the outfall is completed and before any effluent is discharged into the outfall. Beside that, the denser seawater always enters into the sea outfall through the diffuser ports to replace effluent in the tunnel whenever the effluent discharge decreases. The presence of seawater may cause a reduction of the hydraulic efficiency of the sea outfall (Bennet 1981, Munro D. 1981, and Charlton 1982a).

The seawater in the tunnel forms a saline wedge which may block the effluent discharge from risers located seaward of the wedge. This mechanism is known as saline wedge blocking (Figure 2.6b). Intrusion of seawater into the tunnel may occur through some risers. This will mix with effluent in the tunnel and discharge back through another riser. This circulation is called seawater circulation (Figures 2.6a and 2.6c). The two mechanisms of saline intrusion may reduce the effluent discharge.

The process of purging in the sea outfall can be explained using Figure 2.6. The effluent discharge increases slowly from zero through the tunnel and escapes from first riser. As the effluent discharge increases, circulation blocking occurs (Figure 2.6a). The flow in the first riser is a mixture of effluent and seawater drawn into the outfall in downstream risers. This process occurs continually until the sewage discharge increases to a critical flow when there is no circulation blocking in the sea outfall (Figure 2.6b). In this condition, saline wedge blocking occurs in the sea outfall. After that, the purging process moves to the second riser. The circulation blocking occurs between the second riser and the risers located downstream (Figure 2.6c). Complete purging occurs when the effluent discharges through all the risers (Figure 2.6d).

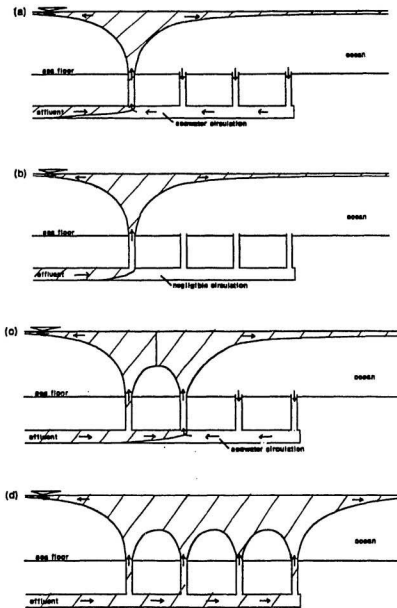


Figure 2.6. Effluent discharge from sea outfall at various stages of purging

The mechanism of seawater circulation and saline wedge blocking in sea outfalls was explained by Wilkinson (1984, 1985). The magnitude of the circulation was obtained in terms of the sewage flow and geometric parameters of the outfall.

The purging discharge depends primarily on the riser height to diameter ratio (h/d) and the diameter of tunnel and riser ratio (D/d). The decrease of tunnel and riser port diameter ratio (D/d) for a tunnel of given cross-sectional area and depth will decrease the purging discharge. In other words, the reduction of the riser diameter (increasing the ratio of D/d) causes a decrease of the purging discharge (Wilkinson 1984).

Wilkinson (1985) derived a nondimensional equation in terms of an outfall Froude number. The equation can be expressed as

$$F_c = \left[\frac{2}{1 + \psi} \right]^{1/2} \quad (2.75)$$

in which

$$F_c = \frac{Q_c}{a(\Delta gh)^{1/2}} \quad (2.76)$$

where

F_c = critical outfall densimetric Froude number

Q_c = critical effluent discharge required to purging of outfall

a = total cross-sectional area of ports on a single riser

$\Delta = (\rho_s - \rho_f) / \rho_f$

ρ_s = seawater density

ρ_e = effluent density

g = acceleration of gravitational

h = height of riser ports above tunnel centerline

ψ = friction factor of riser

Equation 2.75 can be modified in terms of the port densimetric Froude number F_p and the riser height to port diameter (h/d) ratio by multiplying both sides of Equation 2.75 by $(h/d)^{1/2}$ to give

$$F_p = \left(\frac{2}{1 + \psi} \cdot \frac{h}{d} \right)^{1/2} \quad (2.77)$$

in which

$$F_p = \frac{Q_c}{a(\Delta g d)^{1/2}} \quad (2.78)$$

Wilkinson (1988) recommended the effluent flow to purge the seawater for the uniform pipe diameter as

$$Q > \left(\frac{2D \left(\frac{\Delta \rho}{\rho} \right) g \sin \theta}{f} \right) \frac{\pi D^2}{4} \quad (2.79)$$

where

Q = effluent flow required to purge outfall

D = tunnel diameter

$\Delta\rho$ = density difference between seawater and effluent = $\rho_s - \rho_e$

ρ_s = density of seawater

ρ_e = density of effluent

g = acceleration of gravitational

θ = tunnel slope

f = tunnel friction factor

Wilkinson (1991) stated that seawater circulation reduces the hydraulic efficiency of a sea outfall which may then become blocked by accumulated sediments and marine growth. The basic design consideration for sea outfalls with long risers is the ability to purge. In this paper, Wilkinson developed model scaling laws based on the interaction between physical and purging process. This included fluid inertia, buoyancy, friction and entrainment.

2.4. Prevention of seawater intrusion

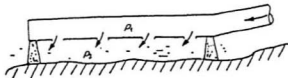
Seawater intrusion in outfalls cannot be stopped if the effluent discharge is not enough to purge. In this condition, the prevention of intrusion or the ability to purge seawater using low effluent discharges is very important.

Charlton (1985a) suggested some ways to control and prevent seawater intrusion into a sea outfall. Firstly, the face of ports could be oriented downward and the ports can be used for a horizontal diffuser section of pipe outfall that is located above the sea floor (Figure 2.7a). Secondly, a separation weir could be used in diffuser heads (Figure 2.7b). Thirdly, flexible duck-

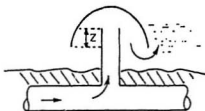
bill discharge valves could be used (Figure 2.7c). Fourthly, a venturi shaped outlet port could control primary intrusion (Figure 2.7d). Fifthly, a venturi control in the tunnel will control the accumulation of seawater in the tunnel (Figure 2.8b). Sixthly, a cranked tunnel-diffuser could be used to block the intrusion of seawater in the tunnel (Figure 2.7e).

Charlton (1985b) presented two types of venturi control. The venturi controls are Venturi control Mk I (Figure 2.8a) and Venturi control Mk II (Figure 2.8b). These can control the seawater intrusion at 50 % of the dry weather flow (DWF). Venturi control Mk I is the same as Venturi Mk II in the throat cross-sectional area, but different in shape. Control Mk I has a circular cross-section shape while control Mk II is vertical sided. For design purposes, Charlton suggested that a densimetric Froude (F_d) = 0.5 should be used.

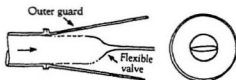
a.



b.



c.



d.



e.

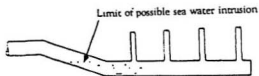
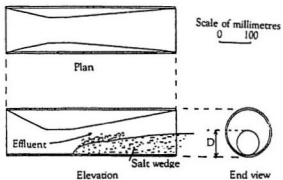


Figure 2.7. a. An intrusion proof diffuser, b. An intrusion proof head, c. Anti-intrusion flexible 'duck-bill' valve, d. A venturi shaped outlet port, and e. A cranked tunnel-diffuser (Charlton, 1985a).

a.



b.

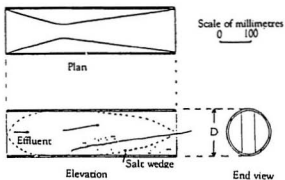


Figure 2.8. a. Venturi control Mk I-circular section, asymmetric (Charlton, 1985b) and b. Venturi control Mk II-vertical sided (Charlton, 1985a and Charlton, 1985b).

Chapter 3

Laboratory Study

3.1. Purpose and general outline of study

The processes involved in purging a tunnelled outfall were modelled and studied in the Hydraulics Laboratory of Memorial University of Newfoundland. Two types of experiments were conducted. The first set of experiments was designed to investigate the effect of discharge port area on the flow in the tunnel. Accordingly tests were run on uncapped risers and compared with tests on capped risers having one port and having two ports. The other experiments were designed to find ways in which the tunnel purging discharge might be reduced. Initially it was thought that air injected below the risers might be beneficial because it would establish an initial upward flow in the riser. It was then realised however that there would be significant practical problems in pumping air down into the tunnel which might be over 100 m below the sea level (the Boston tunnel is approximately 150 m below sea level). Because there is less density

difference between fresh and salt water than between air and salt water, these practical problems would be of lesser magnitude if freshwater were to be injected beneath the risers. This would also initiate a vertical flow and might be more practicable. Both alternatives were tried. It was also considered that anything which reduced stratification in the tunnel upstream of the risers might be beneficial. Accordingly tests were undertaken with freshwater injected into the tunnel upstream of the risers. Finally attempts were made to break down the stratification using a barrier set in the roof of the tunnel and designed to cause the freshwater effluent to plunge down into the salt water sitting in the bottom part of the tunnel.

A general outline of the laboratory study is given here. Section 3.2 describes the experimental facilities used in this study. The experimental procedures are presented in section 3.3 which contains general information about the experimental procedure, saltwater preparation, test procedures, and recording of results.

3.2. Experimental facilities

The main facilities of this study were a sea tank, tunnelled outfall, pump, cylindrical tank, and various flowmeters. The facilities can be seen in Figures 3.1 and 3.2.

The sea tank was 8500 mm long by 1000 mm wide and 1000 mm deep, with one transparent side (3400 mm x 850 mm) to facilitate viewing when the experiment was in progress. It was supported on a substantial steel structure that also incorporated the flowmeters and the saltwater preparation platform (1220 mm x 570 mm). The sea tank



Figure 3.1. Photograph of the experimental facilities

was fitted with an overflow to maintain a constant water level.

A model of the tunnelled outfall was constructed with the tunnel section located below the sea tank. Four riser pipes connected the tunnel to the floor of the sea tank which simulated the sea floor. The inside diameters of the tunnel and the risers were 146 mm (5.75 inches) and 57 mm (2.25 inches) respectively. The tunnel and the four riser pipes were made from a clear acrylic pipe to aid visual studies of fluid flows and fluid mixing. The clear acrylic pipes were linked to the pump and the circular tank with an opaque pipe.

Freshwater and saltwater were discharged to the test tank using a pump (Gould Century, model # 3D11/2-S). Beside that, the pump was also required to mix freshwater

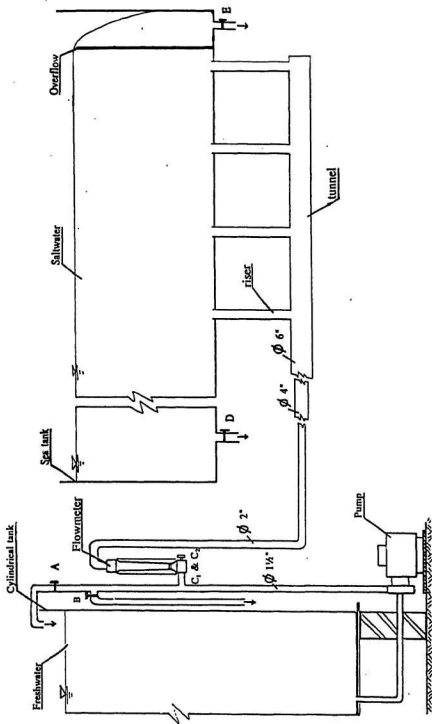


Figure 3.2. Experimental facilities

and salt in the circular tank, and to drain the remaining saltwater and freshwater from the circular tank. The use of the pump will be explained in sections 3.3.2 and 3.3.3.

A fiberglass cylindrical tank with capacity 2273 litres (500 imperial gallons), 1219 mm (48 inches) inside diameter and 2133 mm (84 inches) deep, was used to facilitate the freshwater and saltwater preparation. The freshwater and saltwater preparation will be explained more detail in section 3.3.2 and 3.3.3. This tank was also used as a supply tank for the freshwater effluents.

Three types of flowmeter were used in the experiments. Firstly, two flowmeters were located between the pump and the tunnel to measure the discharge of freshwater from the circular tank (Figure 3.3). The flowmeters used were rotameters (Fischer & Porter, model # 10A3555A) and consisted of a steel float within a glass tube. The range of the flowmeter was from 20 % to 100 % of the maximum discharge (30 US GPM). Secondly, four flowmeters were used to measure the freshwater discharge from the freshwater source to a nozzle located below each riser (Figure 3.4). Each of these flowmeters (Fischer & Porter, model # 10A6731N) consisted of a valve and a steel bubble within a glass tube. The range was 20 % to 100 % of the maximum discharge (29 US GPH). Thirdly, one flowmeter was located between the freshwater source and a nozzle located upstream of the risers (Figure 3.5). The flowmeters (Fischer & Porter, model # FP-1/2-21-G-10/77) used were rotameters. The range was 0.2 l/min to 2.4 l/min.

A portable conductivity/salinity meter (YSI Incorporated, model # YSI Model 33) was used to measure the density of saltwater during the saltwater preparation in the



Figure 3.3. Photograph of the flowmeters model # 10A3555A



Figure 3.4. Photograph of the flowmeters model # 10A6731N



Figure 3.5. Photograph of the flowmeter model # FP-1/2-21-G-10/77

circular tank. The salinity meter had a measuring range from zero to forty parts/thousand.

3.3. Experimental procedure

3.3.1. General

Experiments on the purging of the tunnel were done using the main facilities described earlier in section 3.1. Two types of experiments were conducted. The first was to determine the effect of port size. The second was to identify the mechanism by which mixing occurred, and by which circulation blocking might develop and finally be purged.

The purging discharge experiments were conducted using various combinations of freshwater discharge in the tunnel to simulate the effluent flow, various densities of saltwater in the sea tank as simulation of sea water, and installation of varying additional equipment to increase the mixing of saltwater and freshwater in the tunnel.

A dye was used in these experiments to aid visual observation of mixing between the saltwater and freshwater in the tunnel. The dye was mixed with freshwater in the cylindrical tank using the pump. Two types of dye were used in these experiments. These were Potassium Permanganate (P-278) from Fisher Scientific Company and 07209 Amaranth Supra from Warner Jenkinson (Canada) Limited. The Potassium Permanganate was used in the early experiments on the effect of port size. Beside that, it was also used for the experiments using the water jets located below the risers. However due to the corrosion characteristics of the Potassium Permanganate, it was

changed for food dye (07209 Amaranth Supra) in later experiments.

Discharges used ranged from 11.36 to 68.14 l/min. Density of the saltwater in the sea tank was varied from 1.010 to 1.020 g/cm³.

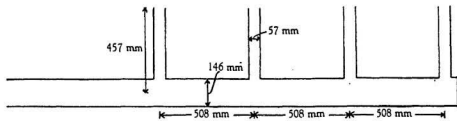
The types of experiments that were used in the purging discharge study are described here.

- a). The main system consisted of the tunnel of internal diameter 146 mm (5.75 inches) and four risers with internal diameter 57 mm (2.25 inches). The height of each riser from the centre of the main tunnel was 457 mm (18 inches). The distance between risers was 508 mm (20 inches). This can be seen in Figure 3.6a.
- b). Experiments were also conducted on risers fitted a cap, each cap having two ports at the head of the risers. The ports were 25.4 mm (1 inch) in diameter. The height of the port centre from the centre of the main tunnel was 489 mm (19.25 inches). This is shown in Figure 3.6b.
- c). Tests were then made with only one port in the riser cap. Again the port was 25.4 mm (1 inch) in diameter. This is shown in Figure 3.6c.

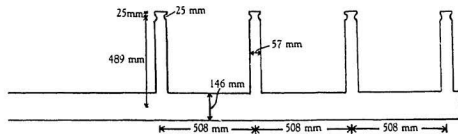
All other tests related to attempts to increase mixing in order to decrease the discharge at which all ports were purged of saltwater. Various ways were used to increase mixing. These included small water jets located beneath the risers or in the tunnel upstream of the risers. Air jets were also investigated and finally a barrier was constructed across the top of the tunnel.

d). Small pipes with internal diameter 2 mm (0.1 inch) were used to release a freshwater

a.



b.



c.

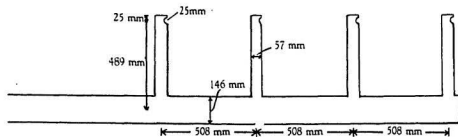


Figure 3.6. a. Risers with no caps; b. Risers with caps, each with two ports; and c. Risers with caps, each with one port.

discharge into the tunnel. These water jets were located below the risers in the tunnel (Figure 3.7a).

e). A water jet was also located upstream of the risers in the tunnel to increase the mixing of saltwater and freshwater (Figure 3.7b). The diameter of this small pipe was 2 mm (0.1 inch). Three different distances from the first riser were used. These were 508 mm (20 inches), 762 mm (30 inches), and 1524 mm (60 inches).

f). The four small pipes below the risers were also used to discharge air (Figure 3.7c).

g). A barrier was located across the tunnel and upstream of the first riser (Figure 3.7d). The barrier is 635 mm (25 inches) from the first riser to the centre of the barrier, and 45° slope and 73 mm (2.875 inches) height to the top wall tunnel .

3.3.2. Saltwater preparation

Saltwater was prepared in a cylindrical tank by mixing freshwater and powdered salt (Figure 3.8). This saltwater was used to simulate seawater. Before mixing the saltwater mixture, all the valves (valve A, B, C₁ and C₂, see Figures 3.2 and 3.8) were closed and the cylindrical tank was filled with freshwater to 175 cm depth. After that, the salt powder was poured by hand from the platform. The freshwater and salt were mixed using a pump and opening control valve 'A' located between the pump and the circular tank (see Figures 3.2 and 3.8). The amount of salt powder to be added in the tank was done step by step until the required density of saltwater was reached, for instance 1.010, 1.015, or 1.020 g/cm³. The density of the saltwater was measured using the salinity meter. After the saltwater was prepared, control valve 'A' was closed and the

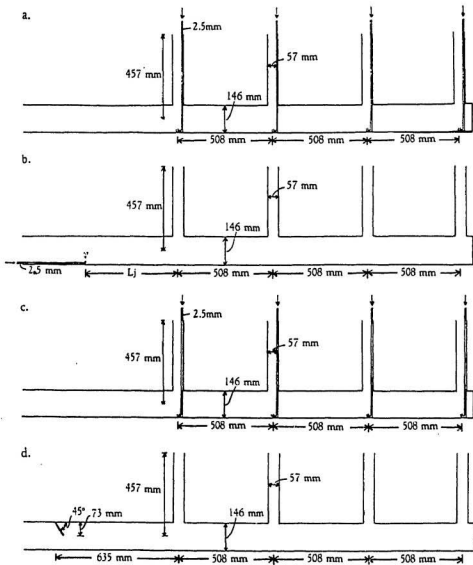


Figure 3.7. a. Water jets located below risers; b. Water jet located upstream of risers; c. Air jets located below risers; and d. Top barrier located upstream of risers.

pump was turned off. All the valves (A, B, C₁, C₂, D, E and F, see Figures 3.2 and 3.8) in the experimental facilities were closed and then the pump and the control valves 'C₁' and 'C₂' located between the pump and the tunnel, were opened to discharge the saltwater to the sea tank (see Figures 3.2 and 3.8). This process was done one time to get the lowest depth of the saltwater in the sea tank (ie. 309 mm) and two times for the highest depth (ie. 605 mm).

After the saltwater in the sea tank was sufficiently deep, the control valves 'C₁' and 'C₂' (see Figures 3.2 and 3.8) were closed. The remaining saltwater in the circular tank was drained using the pump and opening control valve 'B' (see Figure 3.2) located between the pump and the drain. The circular tank was cleaned with freshwater. This process was done until all saltwater was flushed out and changed with new freshwater.

3.3.3. Test procedure

Initial tests were run on the basic system consisting of the main tunnel of internal diameter 146 mm and four risers of internal diameter 57mm (see Figures 3.2 and 3.6a). The risers had no caps. The saltwater ($\rho_s = 1.010 \text{ g/cm}^3$) that was prepared in the circular tank (section 3.3.2) was discharged into the sea tank to simulate the tunnel flooded with sea water due to the intrusion of the sea water. The depth of the saltwater in the sea tank (y) was 605 mm. After that, the circular tank was filled with freshwater and a dye (Potassium Permanganate P-278) was mixed into the freshwater. The dyed freshwater was used to simulate sewage that flows into the sea through the sea outfall.

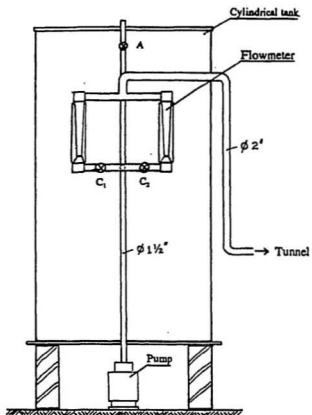


Figure 3.8. Schematic of saltwater preparation

A camera (Pentax PC-505), tripod and three Halogen lamps were prepared to take photographs of the formation and movement of the effluent in the tunnel. The recording of the photographs will be explained more detail in section 3.3.4.

The pump was turned on and control valve 'C₁' (see Figures 3.2 and 3.8) located between the pump and the tunnel, was opened to discharge the dyed freshwater from the cylindrical tank to the sea tank through the flowmeter. The control valve 'E' (see Figure 3.2) located at the edge of the sea tank, was opened to drain the saltwater in the sea tank and maintain a constant level using an overflow weir at the end of the tank. The discharge of the dyed freshwater was metered through the flowmeter at 10% (minimum discharge of the flowmeter = 10% x 30 US gpm = 11.36 l/min). The dyed freshwater mixed with the saltwater in the tunnel and flowed through the first and second risers (Appendix A, Figure A.1). Due to the difference in density of the fluids, the location of the wedge and the interface between the freshwater ($\rho_f = 1.000 \text{ g/cm}^3$) and saltwater ($\rho_s = 1.010 \text{ g/cm}^3$) in the tunnel were clearly visible. The dyed freshwater gave additional contrast when taking photographs. Photographs were taken after the mixture became stable. Then the discharge of the dyed freshwater was increased until the freshwater started to move from the second riser (Appendix A, Figure A.2). The discharge of the freshwater was increased to 20% (20% x 30 US gpm = 28.39 l/min). Photographs were taken and the dyed freshwater was increased again until the dyed freshwater reached the third riser (Appendix A, Figure A.3). The flowmeter showed 32% (32% x 30 US gpm = 36.34 l/min). At this condition photographs were taken again. The discharge of the dyed freshwater was increased gradually until the dyed freshwater

moved from the third riser (Appendix A, Figure A.4). The flowmeter showed 35% ($35\% \times 30 \text{ US gpm} = 39.75 \text{ l/min}$). At this condition, the dyed freshwater discharged through the first, second and third riser. The dyed freshwater was increased again to reach the fourth riser, but the dyed freshwater still discharged through only the first three risers (Appendix A, Figure A.5). The discharge of dyed freshwater was 48% ($48\% \times 30 \text{ US gpm} = 54.51 \text{ l/min}$). The dyed freshwater was increased until the flowmeter showed 60% ($60\% \times 30 \text{ US gpm} = 68.14 \text{ l/min}$). At this condition, the dyed freshwater still flowed through the three risers (Appendix A, Figure A.6) but not the fourth. The dyed freshwater discharge was stopped when the saltwater was purged from all four risers at 67% (67% of the 30 US gpm = 76.08 l/min) (Appendix A, Figure A.7). The discharges of dyed freshwater here were used as reference for the following experiments.

After full purging of the saltwater occurred, the pump and control valve 'C₁' (see Figures 3.2 and 3.8) were turned off. The saltwater in the sea tank was drained by opening control valve 'D', 'E', and 'F' (see Figure 3.2). The remaining dyed freshwater in the cylindrical tank was flushed out using the pump and with control valve 'B' (see Figure 3.2) open.

The same procedures were done for the following tests:

- 1). Risers with no caps (Figure 3.6a)

These tests were run with densities of saltwater (ρ_s) 1.010, 1.015, 1.020 g/cm³. The height of risers and depth of saltwater used were 457 mm and 605 mm respectively. The

effluent went up through all risers depending on the difference in densities between saltwater and freshwater ($\Delta\rho$). The purging discharge occurred at 76.08, 93.12, and 105.61 l/min when the densities of saltwater were 1.010, 1.015, and 1.020 g/cm³ respectively (see Table 3.1). Although effluent discharged through all the risers, the saltwater was still left in the tunnel in a layer along the bottom (Details of the saline wedge profiles are shown in Appendix B, Figures B.1 and B.2).

2). Risers with caps, each with two ports (Figure 3.6b)

A diffuser cap with two ports, each of diameter 25.4 mm (1 inch) was put at the head of each riser. The caps were set up before the tank was filled with saltwater. Then the saltwater (ρ_s) that was prepared in the circular tank, was discharged into the sea tank. The two saltwater densities used were 1.010 and 1.020 g/cm³. The depths of the saltwater in the sea tank (y) were 309 mm and 574 mm. The purging discharge occurred at 24.98 and 36.34 l/min with saltwater densities were 1.010 and 1.020 g/cm³ respectively (see Table 3.1). The saline wedge profiles in the tunnel for different discharges were very similar to each other. Although the effluent discharged through all the risers, saltwater was still left in the tunnel (see Appendix B, Figure B.3).

3). Risers with caps, each with one port (Figure 3.6c)

A diffuser cap with one port of diameter 25.4 mm (1 inch) was put at the head of each riser. The depth of the saltwater in the sea tank (y) was 574 mm. Two densities were used (1.010 and 1.020 g/cm³). The purging discharge in the tunnel occurred at

12.49 and 22.71 l/min for the saltwater densities of 1.010 and 1.020 g/cm³ respectively (see Table 3.1). The saline wedge profiles in the tunnel for different effluent discharges were very close to each other. Saltwater was still left in the tunnel although the effluent was discharged through all risers (see Appendix B, Figure B.4).

4). Water jet located below the risers (Figures 3.7a and 3.9)

A small pipe with internal diameter 2 mm (0.1 inch) was put into every riser as shown in Figures 3.7a and 3.9. These small pipes were connected to the flowmeters model # 10A6731N operated by control valves, H₁, H₂, H₃, and H₄ (see Figure 3.9). All flowmeters were combined at a brass pipe which was connected to the freshwater source with a plastic pipe.

Ten kinds of experiment were done to study the effect of these jets. First a jet was located only under one riser. Tests were run with the jet under the first, then the second, third and fourth risers. Then jets were located under two consecutive risers and each combination (1 and 2, 2 and 3, 3 and 4) were tested. Jets were then placed under any three consecutive risers and then at all four risers. Each jet discharge was 1 l/min of freshwater. The discharge condition was set by arrangement of the four control valves, H₁, H₂, H₃, and H₄ (see Figure 3.9). For example, the freshwater at the first small pipe was discharged by turning on the first control valve (H₁).

Dyed freshwater in the tunnel was run at 11.36, 28.39, 36.34, 39.75, 54.51, and 68.14 l/min, except when discharging freshwater through all small pipes (ie. under each

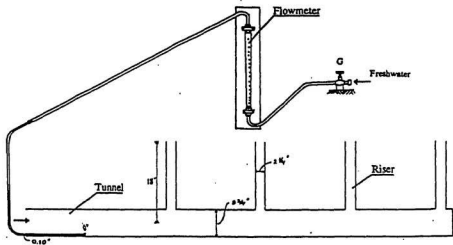


Figure 3.10. Schematic of the experiment with water jet located upstream of the risers in the tunnel

FP-1/2-21-G-10/77 and control valve 'G' (see Figure 3.10). The distance of the nozzle from the first riser was 508 mm (20 inches). The depth of the saltwater in the sea tank (y) was 605 mm.

Experimental procedure was the same as before, except that the water jet of 1 l/min was discharged continually during the experiment by opening valve 'G'. Photographs were taken after the flow became stable. All the procedures were repeated for other dyed freshwater discharges and other distances of water jet (762 mm and 1524 mm) from the first riser.

Effluent was purged through all risers at 71.54 l/min when the distance of the water jet from the first riser was 605 mm and constant at 70.41 l/min when the distances were 762 mm and 1524 mm (see Appendix B, Figures B.15 to B.17).

6). Air jets located below the risers (Figures 3.7c and 3.11)

Small pipes were connected to control valves (I_1 , I_2 , I_3 , and I_4) fitted to a common steel pipe (Figure 3.11). The steel pipe was connected to a pressured air source with a rubber pipe. Air was released into the flow through small pipes using control valves (I_1 , I_2 , I_3 , and I_4).

The process of the experiment was same as for the experiments with water jets located below the risers, except that all the air jets were discharging continually during

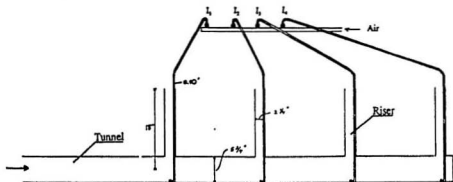


Figure 3.11. Schematic of the experiment with air jets located below the risers in the tunnel

the experiment. Each discharge of air was measured using a calibrated beaker with capacity 1 litre and a stopwatch (Figure 3.12). The beaker was connected to an aluminum stick to reach the hole of the riser. By knowing the volume of air in the beaker and the time of collection, the rate of discharge of air could be calculated. The air jets run at the first, second, third and fourth risers were 0.025, 0.026, 0.028, and 0.028 l/min respectively. It was not possible to maintain the same flow in all air jets due to the problem of adjusting the control valves (I_1 , I_2 , I_3 , and I_4).

Saltwater discharged through all risers when the effluent purging discharge was 68.14 l/min (see Appendix B, Figure B.18).

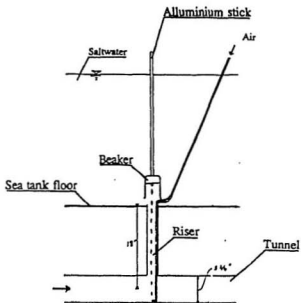


Figure 3.12. Schematic of the air bubble measuring

7). Top barrier located upstream of the risers (Figure 3.7d)

A barrier was located across the top of the tunnel and upstream of the risers with the intention of increasing the mixing between saltwater and effluent.

The barrier was 635 mm (25 inches) from the first riser. The depth of the saltwater in the sea tank (y) was 605 mm. Saltwater in the tunnel was purged at an effluent discharge of 68.14 l/min for a density difference of 0.010 g/cm³ (see Appendix B, Figure B.19).

A summary of all these tests is shown in Table 3.1.

3.3.4. Recording of results

As mentioned earlier, this study used photography to record the movement of the effluent in the tunnel. The camera (Pentax PC-505), including tripod, three Halogen lamps, and a photograph label, had to be prepared and set up before the photographs were taken (Figure 3.13). The photograph label consisted of the date of the experiment, number of ports (n), diameter of port (d), diameter of tunnel (D), depth of riser between tunnel centre and edge of riser or port centre (h), density difference between saltwater and dyed freshwater ($\Delta\rho$), and discharge of dyed freshwater (Q_1). The label also gave information about the position of the jet and the discharge of the jet (Q_2) for water jets located beneath the risers or the distance of the water jet (L_j) for a water jet located upstream the risers. These labels were included in the photographs to ensure that all photographs were clearly identified.

Test No.	Type of Test	Diameter of Port d, mm	Diameter of Jet d_j , mm	Depth of Riser h, mm	Depth of Saltwater y, mm	Density of Saltwater ρ_s , g/cm ³	Density of Effluent ρ_e , g/cm ³	Range of Effluent Discharge Q_1 , l/min	Jet Discharge Q_2 , l/min
1.1	Risers having no caps	-	-	457	605	1.010	1.000	11.36 - 76.08	-
1.2	Risers having no caps	-	-	457	605	1.020	1.000	11.36 - 105.61	-
1.3	Risers having no caps	-	-	457	605	1.015	1.000	11.36 - 93.12	-
2.1	Risers having caps, each with two ports	25	-	489	574	1.010	1.000	11.36 - 24.98	-
2.2	Risers having caps, each with two ports	25	-	489	309	1.020	1.000	11.36 - 36.34	-
3.1	Risers having caps, each with one port	25	-	489	574	1.010	1.000	11.36 - 12.49	-
3.2	Risers having caps, each with one port	25	-	489	574	1.020	1.000	11.36 - 22.71	-
4.1	Water jet located at first riser	-	3	457	605	1.010	1.000	11.36 - 68.14	1.00
4.2	Water jet located at second riser	-	3	457	605	1.010	1.000	11.36 - 68.14	1.00
4.3	Water jet located at third riser	-	3	457	605	1.010	1.000	11.36 - 68.14	1.00
4.4	Water jet located at fourth riser	-	3	457	605	1.010	1.000	11.36 - 54.51	1.00
4.5	Water jets located at first and second risers	-	3	457	605	1.010	1.000	11.36 - 68.14	1.00
4.6	Water jets located at second and third risers	-	3	457	605	1.010	1.000	11.36 - 68.14	1.00
4.7	Water jets located at third and fourth risers	-	3	457	605	1.010	1.000	11.36 - 54.51	1.00
4.8	Water jets located at first, second and third risers	-	3	457	605	1.010	1.000	11.36 - 68.14	1.00
4.9	Water jets located at second, third and fourth risers	-	3	457	605	1.010	1.000	11.36 - 54.51	1.00
4.10	Water jets located at first, second, third and fourth risers	-	3	457	605	1.010	1.000	11.36 - 36.34	1.00
5.1	Water jet located upstream of first riser, $L_j = 508$ mm	-	3	457	605	1.010	1.000	11.36 - 71.54	1.00
5.2	Water jet located upstream of first riser, $L_j = 762$ mm	-	3	457	605	1.010	1.000	11.36 - 70.41	1.00
5.3	Water jet located upstream of first riser, $L_j = 1524$ mm	-	3	457	605	1.010	1.000	11.36 - 70.41	1.00
6.1	Air jets located at first, second, third and fourth risers	-	3	457	605	1.010	1.000	11.36 - 61.14	$Q_{11} = 0.025$ $Q_{12} = 0.026$ $Q_{13} = 0.028$ $Q_{14} = 0.028$
7.1	Top barrier located upstream of first riser	-	-	457	605	1.010	1.000	11.36 - 70.41	-

Note:

In all experiments, tunnel diameter = $D = 146$ mm

riser diameter = $d = 37$ mm

number of riser = $n = 4$

Table 3.1. Summary of test procedures

Three photographs were taken after the mixture of saltwater and dyed freshwater became stable at the required flow. In the first, the camera was located at position A (see Figure 3.13). Then it was moved to position B and position C. At every position, a photograph was taken. This procedure was done for all freshwater discharges studied. The three photographs were enough to cover the whole of the tunnel. After the film was complete, it was developed. Results were transferred to tracing paper after the photographs were combined in their proper order. A typical set of three photographs is shown in Figure 3.14. Results are shown in Appendix A and B.

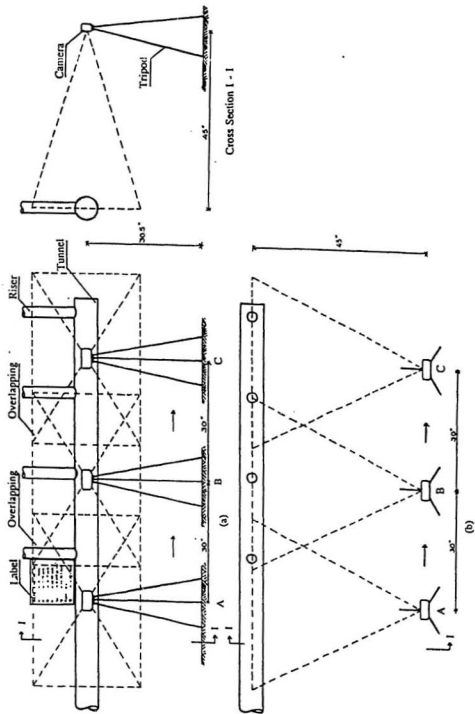


Figure 3.13. Recording procedures. a. Front view, and b. Plan view

Chapter 4

Results and Discussion

4.1. General

The results of the tests are divided into two parts. These are the results of the effect of port size and the results of attempts to increase mixing between the saltwater and the effluent mixture. Experimental results are shown in Tables 4.1 to 4.10, Figures 4.1 to 4.3, Appendix A, and Appendix B.

The results of the port size effect (Tables 4.1 and 4.2) are plotted to show a relationship between the densimetric Froude number at the port, F_p , and tunnel diameter to port diameter, D/d in Figure 4.1. In Figure 4.2, the densimetric Froude number at the port, F_p , is plotted against the ratio height of the riser to port diameter, h/d . A plot is also given of the critical densimetric Froude number, F (Wilkinson, 1985) against tunnel diameter to port diameter, D/d in Figure 4.3. In addition, the condition of flow in the risers and the saline wedge profiles throughout these tests are shown in Tables 4.3 to 4.6,

Appendix A Figures A.1 to A.7, and Appendix B, Figures B.1 to B.4.

The conditions of flow in the risers using various methods to increase mixing in the tunnel and promote flows in the risers are shown in Tables 4.7 to 4.10. The saline wedge profiles in the tunnel for these experiments also can be seen in Appendix B. Figures B.5 to B.14 give data for water jets located below risers; Figures B.15 to B.17 give data for water jets located upstream of risers; Figure B.18 shows results for air jets located below risers, and Figure B.19 shows the effect of a barrier located at the top of the tunnel and upstream of the risers.

Initial tests described in section 3.3.3 were run on the basic system to establish purging flows and basic salinity profiles both of which could be used for comparison with modifications (eg. caps, use of jets, barrier, etc) to the basic system. The tests were run using a density difference of 0.010 g/cm^3 and flows varying from 11.36 l/min to the discharge at which the tunnel was purged 76.08 l/min. The shapes of the saline wedges at these different flows are shown in Figures A.1 to A.7 (Appendix A). These show how the saline wedge progresses along the tunnel as the flow increases and how the risers progressively purge.

4.2. Tests on the effect of port size

The experiments on the effect of port size were done using three types of model. In the first model the risers had no caps. The diameter of each riser was 57.1 mm. The second model had risers provided with caps, each cap having two ports. The diameter

of each port was 25.4 mm. In the third model the risers were fitted with caps having only one port. The diameter of each port was again 25.4 mm.

Data for risers with no caps were taken for three different densities of saltwater, ρ_0 (see Table 4.1). These data were used to calculate the port densimetric Froude number, F_p , the critical densimetric Froude number, F , the ratio of tunnel diameter and port diameter, D/d , and the ratio, height of riser to port diameter, h/d (see Table 4.2). The same calculations were done for the risers fitted with caps having one and two ports.

The port densimetric Froude number, F_p , and the critical densimetric Froude number, F , are defined in terms of the purging discharge by

$$F_p = \frac{Q_p}{4a_i(\Delta g d)^{1/2}} \quad (4.1)$$

and

$$F = \frac{Q_p}{A(\Delta g h)^{1/2}} \quad (4.2)$$

where

F_p = port densimetric Froude number

F = critical densimetric Froude number

Q_p = purging discharge

a_i = total port area per riser

= a , for risers with no caps and risers with cap, each cap with one port

Test No.	Type of Test	Date of Test	Diameter of Port d, mm	Diameter of Tunnel D, mm	Depth of Riser h, mm	Depth of Saltwater y, mm	Density of Saltwater ρ_s , g/cm ³	Density of Effluent ρ_e , g/cm ³	Purging Discharge Q_p , l/min
1	Risers having no caps	16-Dec-93	57	146	457	605	1.010	1.000	76.08
2	Risers having no caps	20-Dec-93	57	146	457	605	1.020	1.000	105.61
3	Risers having no caps	04-Jan-94	57	146	457	605	1.015	1.000	93.12
4	Risers having caps, each with two ports	22-Dec-93	25	146	489	574	1.010	1.000	24.98
5	Risers having caps, each with two ports	23-Dec-93	25	146	489	309	1.020	1.000	36.34
6	Risers having caps, each with one port	21-Dec-93	25	146	489	574	1.010	1.000	12.49

Table 4.1. Data collected on three types of test

Test No.	Type of Test	Area of Port a , x 10 mm	Area of Tunnel A , x 10 mm	Total Area of Ports at Each Riser a_1 , x 10 mm	$\Delta = \frac{\rho_s - \rho_e}{\rho_e}$	D/d	h/d	$F_p = \frac{Q_p}{4a_s(\Delta g d)^{1/2}}$	$F = \frac{Q_p}{A(\Delta g h)^{1/2}}$
1	Risers having no caps	25.65	167.53	25.65	0.010	2.56	8.00	1.65	0.36
2	Risers having no caps	25.65	167.53	25.65	0.020	2.56	8.00	1.62	0.36
3	Risers having no caps	25.65	167.53	25.65	0.015	2.56	8.00	1.65	0.36
4	Risers having caps, each with two ports	5.07	167.53	10.14	0.010	5.75	19.3	2.06	0.11
5	Risers having caps, each with two ports	5.07	167.53	10.14	0.020	5.75	19.3	2.12	0.11
6	Risers having caps, each with one port	5.07	167.53	5.07	0.010	5.75	19.3	2.06	0.06

Note: All test data are taken from Table 4.1

Table 4.2. Analysis of data collected on three types of test

= $2a$, for risers with caps, each cap with two ports

a = area of port = $1/4 \pi d^2$

A = area of tunnel = $1/4 \pi D^2$

Δ = $(\rho_o - \rho_f)/\rho_f$

ρ_o = density of saltwater

ρ_f = density of freshwater

g = gravitational acceleration

d = diameter of port

D = diameter of tunnel

h = height of riser

The results of the tests are plotted in terms of port densimetric Froude number, F_p , against tunnel diameter to port diameter, D/d (see Figure 4.1), port densimetric Froude number, F_p , against height riser to port diameter, h/d (see Figure 4.2), and critical densimetric Froude number, F_c , against tunnel diameter to port diameter, D/d (see Figure 4.3).

As shown in Figure 4.1, Tables 4.1 and 4.2, the values of port densimetric Froude number, F_p , depend on the ratio of the tunnel diameter and riser or port diameter, D/d . For risers have no caps with three different densities of saltwater ($\rho_o = 1.010, 1.015$, and 1.020 g/cm^3) and the ratio of the tunnel diameter and riser diameter, $D/d = 2.56$, the values of port densimetric Froude number F_p are 1.62 and 1.65. The port densimetric Froude number, $F_p = 2.06$ and 2.12 are for the ratio of the tunnel diameter and port

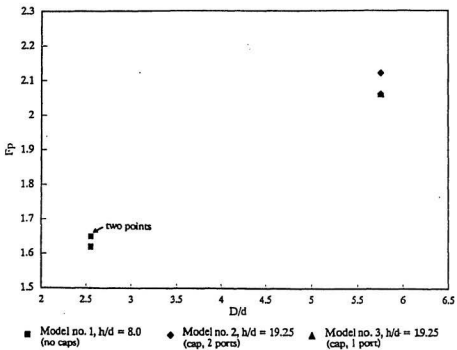


Figure 4.1. Port densimetric Froude number as Function of tunnel diameter to port diameter.

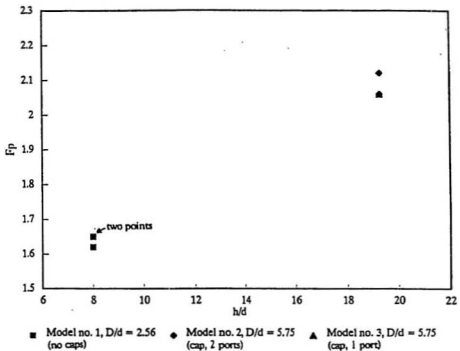


Figure 4.2. Port densimetric Froude number as Function of riser height to port diameter.

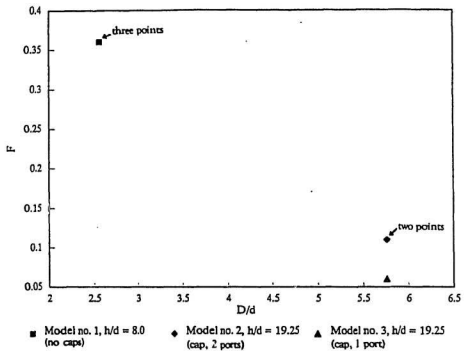


Figure 4.3. Critical densimetric Froude number as Function of tunnel diameter to port diameter.

diameter, $D/d = 5.75$ and the density of saltwater, $\rho_s = 1.010$ and 1.020 g/cm^3 , for risers have caps, each with one port and two ports. From Figure 4.1, it can be seen that the value of port densimetric Froude number, F_p , increased as the ratio of tunnel diameter to port diameter, D/d increased.

From the results of these experiments, it could be concluded that the value of port densimetric Froude number, F_p , depended on the ratio of tunnel diameter to port diameter, D/d . It did not depend directly on the density of saltwater and the number of ports. The port densimetric Froude number increased as the ratio of tunnel diameter to port diameter increased. This implies as expected, that if all other variables are held constant, the purging discharge increases as the tunnel diameter increases. It also suggests that purging discharge increases with density difference if geometric variables are constant.

The correlations between the port densimetric Froude number, F_p , and the height of riser to port diameter, h/d is shown in Figure 4.2, Tables 4.1 and 4.2. The results are the same as those of Figure 4.1, namely that the port densimetric Froude number, F_p , is a function of height of riser to port diameter, h/d . It did not depend on the density of saltwater and the number of ports. The port densimetric Froude number increased as well as the ratio of height of riser to port diameter.

In Figure 4.3, Tables 4.1 and 4.2, the critical densimetric Froude number, F is the function of the ratio of tunnel diameter to port diameter, D/d . The critical densimetric Froude numbers, F are constant for the same type of tests, although the densities of

saltwater, ρ_s are different. As the ratio of the tunnel to port diameter decreased, the critical densimetric Froude number increased. From Table 4.2, the critical densimetric Froude number depended on the total area of ports at each riser, a_r .

The purging discharge, Q_p , increased as the density of saltwater, ρ_s increased with the same effluent density, ρ_e and the same test configuration (see Table 4.1). In the test with risers having no caps and effluent density, $\rho_e = 1.000 \text{ g/cm}^3$, the purging discharges were 76.08, 93.12 and 105.61 l/min for saltwater densities of 1.010, 1.015 and 1.020 g/cm^3 respectively. The purging discharges were 24.98 and 36.34 l/min for saltwater densities of 1.010 and 1.020 g/cm^3 respectively for the tests with risers having caps with two ports and the effluent density of 1.000 g/cm^3 .

The tunnel saline wedge profiles for risers with no cap at the same effluent discharge were different depending on the difference in density between the saltwater and the effluent, $\Delta\rho$. The saltwater left in the tunnel with a density difference of $\Delta\rho = 0.010 \text{ g/cm}^3$ was smaller than with a density difference of $\Delta\rho = 0.020 \text{ g/cm}^3$ at the same effluent discharge (see Appendix B, Figures B.1 and B.2). This means that to purge the saltwater from the tunnel requires a higher effluent discharge for higher density differences.

The condition of flow in risers 1 to 4 for different types of tests (No cap in risers, caps having one port and caps having two ports) but the same density difference ($\Delta\rho = 0.020 \text{ g/cm}^3$) can be seen in Tables 4.3 to 4.6 and Appendix B, Figures B.2 to B.4. These can be explained as follows:

TYPE OF TEST	CONDITION OF FLOW IN RISER # 1		
	Q1 = 11.36 l/min	Q2 = 28.39 l/min	Q3 = 36.34 l/min
No cap in risers	up	up	up
$\Delta\rho = 0.020 \text{ g/cm}^3$ With caps, each with two ports of $d = 25.4 \text{ mm}$ $\Delta\rho = 0.020 \text{ g/cm}^3$	up	up	up
With caps, each with one port of $d = 25.4 \text{ mm}$ $\Delta\rho = 0.020 \text{ g/cm}^3$	up	up	up

Table 4.3. Condition of flow in riser # 1 at same freshwater discharge and density for different numbers of caps and ports

TYPE OF TEST	CONDITION OF FLOW IN RISER # 2		
	Q1 = 11.36 l/min	Q2 = 28.39 l/min	Q3 = 36.34 l/min
No cap in risers	up	up	up
$\Delta\rho = 0.020 \text{ g/cm}^3$ With caps, each with two ports of $d = 25.4 \text{ mm}$ $\Delta\rho = 0.020 \text{ g/cm}^3$	up	up	up
With caps, each with one port of $d = 25.4 \text{ mm}$ $\Delta\rho = 0.020 \text{ g/cm}^3$	up	up	up

Table 4.4. Condition of flow in riser # 2 at same freshwater discharge and density for different numbers of caps and ports

TYPE OF TEST	CONDITION OF FLOW IN RISER # 3		
	Q1 = 11.36 l/min	Q2 = 28.39 l/min	Q3 = 36.34 l/min
No cap in risers $\Delta\rho = 0.020 \text{ g/cm}^3$	down	down	down
With caps, each with two ports of $d = 25.4 \text{ mm}$ $\Delta\rho = 0.020 \text{ g/cm}^3$	down	up	up
With caps, each with one port of $d = 25.4 \text{ mm}$ $\Delta\rho = 0.020 \text{ g/cm}^3$	up	up	up

Table 4.5. Condition of flow in riser # 3 at same freshwater discharge and density for different numbers of caps and ports

TYPE OF TEST	CONDITION OF FLOW IN RISER # 4		
	Q1 = 11.36 l/min	Q2 = 28.39 l/min	Q3 = 36.34 l/min
No cap in risers $\Delta\rho = 0.020 \text{ g/cm}^3$	down	down	down
With caps, each with two ports of $d = 25.4 \text{ mm}$ $\Delta\rho = 0.020 \text{ g/cm}^3$	down	down	up
With caps, each with one port of $d = 25.4 \text{ mm}$ $\Delta\rho = 0.020 \text{ g/cm}^3$	down	up	up

Table 4.6. Condition of flow in riser # 4 at same freshwater discharge and density for different numbers of caps and ports

For all effluent discharges ($Q_1 = 11.36$ l/min, $Q_2 = 28.39$ l/min, and $Q_3 = 36.24$ l/min), the flow went up through risers #1 and 2.

In riser #3, the saltwater intruded into the tunnel for all effluent discharges in the test with no cap and for $Q_1 = 11.36$ l/min in the tests with a cap having two ports of $d = 25.4$ mm. There was no intrusion in any of the tests on caps with one port of $d = 25.4$ mm.

In riser #4, the saltwater intruded into the tunnel for all effluent discharges for tests with no cap in risers. Seawater also intruded for discharges up to 28.39 l/min for caps with two ports of $d = 25.4$ mm, and for discharges up to 11.36 l/min for tests with caps having one port of $d = 25.4$ mm.

As shown in Table 4.6, the saltwater was purged from the outfall at a discharge of 28.39 l/min if the cap was fitted with one port of $d = 25.4$ mm and at 36.34 l/min if the cap was fitted with two ports of $d = 25.4$ mm. If no cap was fitted the purging discharge was greater than 36.34 l/min. It could also be seen that when the flow in all capped risers fitted with one port was upward, some saltwater was still left in the tunnel while the fresh effluent flowed along the top of the tunnel (see Appendix B, Figure B.4).

The saline wedge profiles in the tunnel with risers having no caps can be seen in Appendix A. The length of the saline wedge increased and the height of still saltwater left in the tunnel decreased as the effluent discharge increased. The purging discharge at $\Delta\rho = 0.010$ g/cm³ was $Q_p = 76.08$ l/min.

These experiments showed generally that the port densimetric Froude number,

F_c increased with increase in the ratio of tunnel diameter to port diameter, D/d as well as with the increase of the ratio height of riser to port diameter, h/d . The critical Froude number, F_c increased with decrease in the total area of ports at each riser, a . Even when the risers all flowed full of effluent, some saltwater was still left in the tunnel. This saltwater could cause longterm damage to the sea outfall. In the next section, tests are described which were intended to increase the mixing of effluent and saltwater in the tunnel so that all saltwater could be purged from the tunnel.

4.3. Tests on jets and barrier

This section will explain the results of test designed to promote upward flow in the risers and to increase the mixing between the saltwater and effluent. These tests used water: jets (located below risers and upstream of risers), air jets located below risers, and a barrier located upstream of the risers. The results are shown in Tables 4.7 to 4.10 and Appendix B, Figures B.5 to B.19.

4.3.1. Tests using water jets

The effect of the different locations of the jets may be compared from the data in Tables 4.7 to 4.10. In addition, all data can be compared with the basic system with no jets. In this basic system for $\Delta\rho = 0.010 \text{ g/cm}^3$ the discharge needed to purge all saltwater from the tunnel was 76.08 l/min.

TYPE OF TEST	CONDITION OF FLOW IN RISER # 1					
	Q1 = 11.36 l/min Q2 = 28.39 l/min Q3 = 36.34 l/min Q4 = 39.75 l/min Q5 = 54.51 l/min Q6 = 68.14 l/min					
No jet in risers	up	up	up	up	up	up
$\Delta\rho = 0.010 \text{ g/cm}^3$						
Water jet Q = 1 l/min below riser 1	up	up	up	up	up	up
$\Delta\rho = 0.010 \text{ g/cm}^3$						
Water jet Q = 1 l/min below riser 2	up	up	up	up	up	up
$\Delta\rho = 0.010 \text{ g/cm}^3$						
Water jet Q = 1 l/min below riser 3	up	up	up	up	up	up
$\Delta\rho = 0.010 \text{ g/cm}^3$						
Water jet Q = 1 l/min below riser 4	up	up	up	up	up	up
$\Delta\rho = 0.010 \text{ g/cm}^3$						
Water jet Q = 1 l/min below riser 1 and 2	up	up	up	up	up	up
$\Delta\rho = 0.010 \text{ g/cm}^3$						
Water jet Q = 1 l/min below riser 2 and 3	up	up	up	up	up	up
$\Delta\rho = 0.010 \text{ g/cm}^3$						
Water jet Q = 1 l/min below riser 3 and 4	up	up	up	up	up	up
$\Delta\rho = 0.010 \text{ g/cm}^3$						
Water jet Q = 1 l/min below riser 1, 2 and 3	up	up	up	up	up	up
$\Delta\rho = 0.010 \text{ g/cm}^3$						
Water jet Q = 1 l/min below riser 2, 3 and 4	up	up	up	up	up	up
$\Delta\rho = 0.010 \text{ g/cm}^3$						
Water jet Q = 1 l/min below riser 1, 2, 3 and 4	up	up	up	up	up	up
$\Delta\rho = 0.010 \text{ g/cm}^3$						
Water jet Q = 1 l/min upstream of riser 1, $L_j = 508 \text{ mm}$	up	up	up	up	up	up
$\Delta\rho = 0.010 \text{ g/cm}^3$						
Water jet Q = 1 l/min upstream of riser 1, $L_j = 762 \text{ mm}$	up	up	up	up	up	up
$\Delta\rho = 0.010 \text{ g/cm}^3$						
Water jet Q = 1 l/min upstream of riser 1, $L_j = 1524 \text{ mm}$	up	up	up	up	up	up
$\Delta\rho = 0.010 \text{ g/cm}^3$						
Air jet						
Q ₃₁ = 0.025 l/min						
Q ₃₂ = 0.026 l/min	up	up	up	up	up	up
Q ₃₃ = 0.028 l/min						
Q ₃₄ = 0.028 l/min						
$\Delta\rho = 0.010 \text{ g/cm}^3$						
Top barrier upstream of riser 1	up	up	up	up	up	up
$\Delta\rho = 0.010 \text{ g/cm}^3$						

Table 4.7. Condition of flow in riser # 1 at same freshwater discharge and density for different types of test

TYPE OF TEST	CONDITION OF FLOW IN RISER #3					
	Q1 = 11.36 l/min	Q2 = 28.19 l/min	Q3 = 56.34 l/min	Q4 = 89.71 l/min	Q5 = 143.1 l/min	Q6 = 286.14 l/min
No jet in riser	up	up	up	up	up	up
$\Delta p = 0.010$ g/cm ³	up	up	up	up	up	up
Water jet Q = 1 l/min below riser 1	up	up	up	up	up	up
$\Delta p = 0.010$ g/cm ³	up	up	up	up	up	up
Water jet Q = 1 l/min below riser 2	up	up	up	up	up	up
$\Delta p = 0.010$ g/cm ³	up	up	up	up	up	up
Water jet Q = 1 l/min below riser 3	up	up	up	up	up	up
$\Delta p = 0.010$ g/cm ³	up	up	up	up	up	up
Water jet Q = 1 l/min below riser 4	up	up	up	up	up	up
$\Delta p = 0.010$ g/cm ³	up	up	up	up	up	up
Water jet Q = 1 l/min below riser 1 and 2	up	up	up	up	up	up
$\Delta p = 0.010$ g/cm ³	up	up	up	up	up	up
Water jet Q = 1 l/min below riser 2 and 3	up	up	up	up	up	up
$\Delta p = 0.010$ g/cm ³	up	up	up	up	up	up
Water jet Q = 1 l/min below riser 3 and 4	up	up	up	up	up	up
$\Delta p = 0.010$ g/cm ³	up	up	up	up	up	up
Water jet Q = 1 l/min below riser 1, 2 and 3	up	up	up	up	up	up
$\Delta p = 0.010$ g/cm ³	up	up	up	up	up	up
Water jet Q = 1 l/min below riser 3 and 4	up	up	up	up	up	up
$\Delta p = 0.010$ g/cm ³	up	up	up	up	up	up
Water jet Q = 1 l/min below riser 1, 2, 3 and 4	up	up	up	up	up	up
$\Delta p = 0.010$ g/cm ³	up	up	up	up	up	up
Water jet Q = 1 l/min upstream of riser 1, $L_j = 508$ mm	up	up	up	up	up	up
$\Delta p = 0.010$ g/cm ³	up	up	up	up	up	up
Water jet Q = 1 l/min upstream of riser 1, $L_j = 762$ mm	up	up	up	up	up	up
$\Delta p = 0.010$ g/cm ³	up	up	up	up	up	up
Water jet Q = 1 l/min upstream of riser 1, $L_j = 1524$ mm	up	up	up	up	up	up
$\Delta p = 0.010$ g/cm ³	up	up	up	up	up	up
Air jet $Q_{air} = 0.025$ l/min $Q_{air} = 0.026$ l/min $Q_{air} = 0.028$ l/min $Q_{air} = 0.028$ l/min	up	up	up	up	up	up
$\Delta p = 0.010$ g/cm ³	up	up	up	up	up	up
Top increase upstream of riser 1	up	up	up	up	up	up
$\Delta p = 0.010$ g/cm ³	up	up	up	up	up	up

Table 4.9. Condition of flow in riser # 3 at same freshwater discharge and density for different types of test

4.3.1.1. Water jets located below risers

The condition of flow in riser #1 is shown in Table 4.7 for all effluent discharges ($Q_1 = 11.36$ l/min to $Q_1 = 68.14$ l/min). In all cases the effluent flow was upward. This means that for all discharges tested the effluent always flowed through the first riser due to the pressure of the effluent discharge and because of the density difference between the effluent and saltwater.

In Table 4.8, it can be seen that when the effluent discharge Q_1 was equal to 11.36 l/min, the saltwater intruded through riser #2 for tests with the water jet located below riser #3, riser #4 and below risers #3 and 4. When the effluent discharge Q_1 was equal to 11.36 l/min and water jets were located below riser #1, 2, 1 and 2, 2 and 3, 1, 2 and 3, 2, 3 and 4, and 1, 2, 3 and 4, and for all discharges greater than 11.36 l/min for all tests, the conditions of flow were upward.

The condition of flow was downward in the third riser (see Table 4.9) for effluent discharges of 11.36 l/min and 28.39 l/min in all cases except for the test with water jets located below risers #1, 2, 3 and 4. For an effluent discharge of 36.34 l/min, the flow was upward for tests with water jets located below riser #3, 1, 2 and 3, and 1, 2, 3 and 4, but all others were downward. The effluent went upwards for flows of 39.75 l/min, except for tests with water jets located below riser #4, 1 and 2, and 2, 3 and 4. The riser flow was upward for the effluent discharge equal to, or more than 54.51 l/min.

The condition of flow in riser #4 is shown in Table 4.10. There was no intrusion

TYPE OF TEST	CONDITION OF FLOW IN RISER # 4						PULSING DISCHARGE (%)
	Q1 = 11.55 l/min	Q2 = 28.34 l/min	Q3 = 35.34 l/min	Q4 = 36.71 l/min	Q5 = 34.51 l/min	Q6 = 48.11 l/min	
No jet in nozzles							70.08
Water jet Q = 1 l/min before zone 1							72.28
Water jet Q = 1 l/min before zone 2							72.28
Water jet Q = 1 l/min before zone 3							72.28
Water jet Q = 1 l/min before zone 4					up	up	54.51
Water jet Q = 1 l/min before zone 1 and 2							71.54
Water jet Q = 1 l/min before zone 2 and 3							71.54
Water jet Q = 1 l/min before zone 3 and 4					up	up	54.51
Water jet Q = 1 l/min before zone 1, 2 and 3							70.41
Water jet Q = 1 l/min before zone 1, 3 and 4					up	up	54.51
Water jet Q = 1 l/min before zone 1, 2, 3 and 4			up	up	up	up	34.54
Water jet Q = 1 l/min upstream of nose 1, $L_d = 508$ mm ($\Delta\rho = 0.010$ g/cm ³)							71.54
Water jet Q = 1 l/min upstream of nose 1, $L_d = 763$ mm ($\Delta\rho = 0.010$ g/cm ³)							70.41
Water jet Q = 1 l/min upstream of nose 1, $L_d = 1014$ mm ($\Delta\rho = 0.010$ g/cm ³)							70.41
Air jet Q1 = 0.025 l/min Q2 = 0.026 l/min Q3 = 0.028 l/min Q4 = 0.028 l/min Q5 = 0.028 l/min Q6 = 0.028 l/min ($\Delta\rho = 0.010$ g/cm ³)						up	68.14
Tap before upstream of nose 1 ($\Delta\rho = 0.010$ g/cm ³)							70.41

Table 4.10. Condition of flow in riser # 4 at same freshwater discharge and density for different type of test

when the effluent discharge was greater than, or equal to 36.34 L/min for tests with water jets located below risers #1, 2, 3 and 4. This condition also occurred for tests with water jets located below riser #4, 3 and 4, and 2, 3 and 4 when the effluent discharge was equal to or greater than 54.51 L/min. For other tests, the condition of flow was downward for all flows between 11.36 L/min and 68.14 L/min.

Saline wedge profiles in the tunnel for tests with water jets located below risers are shown in Appendix B, Figures B.5 to B.14. The saline wedge profile is the boundary between saltwater and effluent in the tunnel. The figures also show that the presence of water jets in the tunnel helped to establish upward flow in the risers and was therefore beneficial in reducing the purging discharge.

The changes shown in Tables 4.7 to 4.10 demonstrate the advantages of the small water jets. Riser #1 had upward flow under all conditions. Flow in riser #2 was generally similar except for the tests where intrusion occurred. Flow in riser #3 was generally downwards at low flows (less than 36.34 L/min) except in two cases where the jets were able to reverse the direction of flow. Riser #4 showed the effects of the small jets in a more obvious way. Because the fourth riser is at the end of the tunnel, it is the most difficult to purge. Thus, with no jets installed intrusion occurred at all discharges up to 68.14 L/min. A single water jet installed under riser #4 ensured that no intrusion would occur at flows greater than 39.75 L/min. A jet under each riser ensured that all risers would be purged at discharges greater than 36.34 L/min.

The best results therefore occurred with water jets located under each riser. The

purging discharge was a minimum for this condition. This compared with a purging discharge of 76.08 l/min with no jets installed. The jets therefore caused a 48% decrease in the discharge needed to purge the tunnel.

4.3.1.2. Water jet located upstream of risers

A water jet was located at three different positions in the tunnel (Appendix B, Figures B.15 to B.17). The three positions (L_j) were 508 mm, 762 mm, and 1524 mm upstream of the first riser. The objective of these tests was to increase the mixing between saltwater and effluent upstream of the risers in an endeavour to decrease the purging discharge.

The condition of flow in riser #1 for three different tests was upward (see Tables 4.7 and 4.8).

From Table 4.9 it can be seen that the saltwater intruded through riser #3 into the tunnel for all tests when the effluent discharge was equal to 11.36 l/min. When the flow was increased to 28.39 l/min, the condition of flow was upward when the water jet was located 508 mm upstream risers, but downwards when the jet was further upstream. At flows greater than 28.39 l/min the riser flow was upward for all tests.

The condition of flow in riser #4 was downward for all tests regardless of the flow magnitude (see Table 4.10). This means that the saltwater still intruded into the tunnel. The purging discharges occurred at a flow of 71.54 l/min for $L_j = 508$ mm and 70.41 l/min for $L_j = 762$ mm and 1524 mm (see Appendix B, Figures B.15 to B.17).

The saline wedge profiles (Appendix B, Figures B.15 to B.17) do not show significant mixing caused by the small upstream jet nor did this jet appear particularly beneficial in helping to purge the tunnel.

4.3.2. Tests using air jets

Air jets were used to try to increase the mixing between effluent and saltwater in the tunnel and to promote upward flow in the risers. The results of the experiments are shown in Tables 4.7 to 4.10 and Appendix B, Figure B.18. It was very difficult to maintain a constant air discharge from one test to another. There were therefore three different discharges of air jets. These were 0.025 l/min, 0.026 l/min, and 0.028 l/min. Air jets were located under all risers in every test.

The condition of flow in riser #1 was always upward. Tables 4.7 to 4.10 show that as the flow increased the risers were successively purged. However upward flow in the fourth riser was not obtained until the discharge increased to 68.14 l/min. The air jets were therefore somewhat helpful in the discharge needed to purge saltwater from the outfall but their effect was not as significant as that of the water jets.

4.3.3. Test using a barrier

The last experiment that was done in this study was to use a barrier located upstream of the risers as shown in Appendix B, Figure B.19. The intention again was to promote mixing and therefore reduce the purging discharge. Results are again shown in Tables 4.7 to 4.10 and in Appendix B, Figure B.19. These results show that the barrier

had little beneficial effect. If the first line in each table (basic system, no jets) is compared with the last line (top barrier in place), it will be seen that the barrier had no effect in the flow except in riser #2 where it caused intrusion at the lowest flow. However the total flow needed to purge the tunnel was reduced from 76.08 l/min in the basic system to 70.41 l/min with a barrier.

Chapter 5

Conclusions and Recommendations

5.1. Conclusions

The results of this study are given in the following conclusions.

1. If other variables are held constant, the purging discharge, Q_p , increases as the density difference between saltwater and effluent increases. The amount of saltwater remaining in the tunnel depends on the density difference. This amount is higher when the density difference is higher.
2. If the port area is varied, the value of port densimetric Froude number, F_p , increases with increase in the ratio, tunnel diameter to port diameter ratio, D/d as well as with increase in the ratio, height of riser to port diameter ratio, h/d . Beside that, the critical Froude number in the tunnel, F increases with decrease in the total area of ports at each riser, a .
3. The presence of water jets, an air jet or a top barrier in the tunnel causes an increase in mixing between the saltwater and the effluent mixture. This increase in mixing

reduced the purging discharge compared to the tests without water jets, air jets or the top barrier. The water jets helped considerably to reduce the purging discharge, the air jets only helped a little and the top barrier helped very little.

4. Most water jets located below the risers in the tunnel only gave a small reduction in the purging discharge. This was of the order of 10%. The exception occurred when water jets were located below all risers. The reduction in purging discharge in that case was significant. Water jets below all risers reduced the purging discharge to 36.34 l/min (48%) compared to that without water jets (76.08 l/min) at the same difference density, $\Delta\rho$. This is the best conclusion for the experiments.

5. A jet located upstream of the risers gave only a slight reduction in purging discharge, of the order of 7.5% ($Q_p = 70.41$ l/min for $L_j = 762$ mm and 1524 mm) and 6% ($Q_p = 71.54$ l/min for $L_j = 508$ mm) compared to tests without a water jet (76.08 l/min) at the same difference density, $\Delta\rho$.

6. With air jets located below the risers, the purging discharge was 68.14 l/min. This represents a reduction of the order of 10% compared to tests without air jets. In this experiment, it was very difficult to maintain the same discharges in different tests.

7. Test using a barrier located upstream of the risers gave a reduction of the order of 7.5% ($Q_p = 70.41$ l/min) compared to tests without a barrier.

Generally it may be concluded that water jets located under all four risers were beneficial and had a significant effect in reducing the purging discharge. Other methods tried (air jets, barriers) had some beneficial effect but generally it was fairly minor and not significant.

5.2. Recommendations

According to the results of this study, the experiment using water jets located below all the risers gave the best result. To maximize the benefit, the water jet discharge should be varied to find the flow that results in the maximum reduction in the purging discharge. Flow characteristics should also be measured under varying density difference. Studies may also be done to see whether the use of water jets is reasonable and practical.

References

- Abraham, G. 1963. "Jet Diffusion in Stagnant Ambient Fluid," *Delft Hydraulics Laboratory*, Publ. No. 29, July.
- Abraham, G. 1965. "Horizontal Jets in Stagnant Fluid of other Density," *Proceedings of American Society of Civil Engineers*, Vol.91, No. HY4, pp. 138-154.
- Adams, E.E., Sahoo, D., Liro, C.R., and Zhang, X. 1994. "Hydraulics of Seawater Purging in Tunneled Wastewater Outfall," *Journal of Hydraulic Engineering*, Vol. 120, No. 2, pp. 209-226.
- Agg, A.R., and Wakeford, A.C. 1972. "Field Studies of Jet Dilution of Sewage at Sea Outfalls," *Journal of Institution of Public Health Engineers*, Vol. 71, pp. 126-149.
- Albertson, M.L., Dai, Y.B., Jensen, R.A., and Rouse, H. 1950. "Diffusion of Submerged Jets," *Transactions of American Society of Civil Engineers*, Vol. 115, pp. 639-697.
- Allen, J.H., and Sharp, J.J. 1987. "Environmental Considerations for Ocean Outfalls and Land based Treatment Plants," *Canadian Journal of Civil Engineering*, Vol. 14, pp. 363-371.
- Bennet, N.J. 1981. "Initial Dilution: A Practical Study on Hastings Long Sea Outfall," *Proceedings Institution of Civil Engineers*, Part 1, Vol. 70, February, pp. 113-122.
- Bennet, N.J. 1983. "Design of Sea Outfalls-The Lower Limit Concept of Initial Dilution," *Proceedings Institution of Civil Engineers*, Part 2, Vol. 75, March, pp. 113-121.
- Brooks, N.H. 1960. "Diffusion of Sewage Effluent in an Ocean Current." *Waste Disposal*

- in the *Marine Environment*, E.A. Pearson, ed., Pergamon Press, New York. N.Y.
- Burrows, R., Ali, K.H.M., and Wose, A.E. 1991. "Laboratory Studies of Saline Intrusion, Salt Wedge Formation and Sediment Deposition in Long-Sea Outfalls," *Environmental Hydraulics*, Lee & Cheung, eds., Balkema, Rotterdam, Netherlands, pp. 269-274.
- Charlton, J.A. 1982a. "Salinity Intrusion into Multiport Sea Outfalls." *Proc. 18th Int. Conference on Coastal Engineering*. Capetown. pp. 2376-2385.
- Charlton, J.A. 1982b. "Hydraulic Modelling of Saline Intrusion into Sea Outfalls," *Proceedings International Conference on the Hydraulic Modelling of Civil Engineering Structures*, Coventry, England, September, pp. 349-356.
- Charlton, J.A. 1985a. "Sea Outfalls." *Developments in Hydraulic Engineering* 3, P. Novak, ed., Vol. 3, Elsevier Applied Science Publishers, London, England.
- Charlton, J.A. 1985b. "The Venturi as a Saline Intrusion Control for Sea Outfalls," *Proceedings of Institution of Civil Engineers*, Part 2, Vol. 79, December, pp. 697-704.
- Charlton, J.A., Davies, P.A., and Bethune, G.H.M. 1987. "Sea Water Intrusion and Purging in Multi-port Sea Outfalls," *Proceedings of Institution of Civil Engineering*, Part 2, Vol. 83, March, pp. 263-274.
- Cederwall, K. 1963. "The Initial Mixing on Jet Disposal into a Recipient," *Chalmers Institute of Technology, Hydraulics Division*, Publication No. 14 and 15, Goteburg, Sweden.
- Cederwall, K. 1968. "Hydraulics of Marine Waste Disposal," *Chalmers Institute of*

- Technology, Hydraulics Division, Report no. 42, Goteburg, Sweden.*
- Chen, C.J., and Rodi, W. 1976. "A Review of Experimental Data of Vertical Turbulent Buoyant Jets," Iowa Institute of Hydraulic Research Rep. No. 193.
- Chin, D.A. 1987. "Influence of Surface Waves on Outfall Dilution," *Journal of Hydraulic Engineering*, Vol. 113, No. 8, pp. 1006-1018.
- Davies, P.A., Charlton, J.A., and Bethune, G.H.M. 1988. "A Laboratory Study of Primary Saline Intrusion in a Circular Pipe," *Journal of Hydraulic Research*, Vol. 26, No. 1, pp. 33-48.
- Fan, L.N., and Brooks, N.H. 1966. Discussion of "Horizontal Jets in Stagnant Fluid of Other Density," *Proceedings of American Society of Civil Engineering*, Vol. 92, no. HY2, March.
- Fick, A. 1855. "On Liquid Diffusion," *Philos. Mag.*, Vol. 4, No. 10, pp. 30-39.
- Fischer, H.B., List, E.J., Koh, R.C.Y., Imberger, J., and Brooks, N.H. 1979. "Mixing in Inland and Coastal Waters," Academic Press, New York, N.Y.
- Frankel, R.J., and Cumming, J.D. 1965. "Turbulent Mixing Phenomena of Ocean Outfalls," *Proceedings of American Society of Civil Engineers*, Vol. 91, no.SA2, pp. 33-59.
- Grace, R.A. 1985. "Sea Outfalls-A Review of Failure, Damage and Impairment Mechanisms," *Proceedings of Institution of Civil Engineering*, Part 1, Vol. 80, pp. 553-557.
- Keulegan, G. 1966. "The Mechanics of the Arrested Salt Wedge." *Estuary and Coastline Hydrodynamics*, A.T. Ippen, ed., McGraw-Hill, New York, N.Y.

- Koh, R.C.Y., Brooks, N.H. 1975. "Fluid Mechanics of Wastewater Disposal in the Ocean." *Annual Review of Fluid Mechanics* 7. 187-211.
- Lee, J.H.W., and Cheung, V. 1991. "Mixing of Buoyancy-dominated Jets in a Weak Current," *Proceedings of Institution of Civil Engineering*, Part 2, 91, pp. 113-129.
- Lee, J.H.W., and Neville-Jones, P. 1987. "Initial Dilution of Horizontal Jet in Crossflow," *Journal of Hydraulic Engineering*, Vol. 113, No. 5, pp. 615-629.
- Liseth, P. 1970. "Mixing of Merging Buoyant Jets from Manifold in Stagnant Receiving Water of Uniform Density," *Hydraulics Engineering La. Univ of California*, Berkeley, Tech. Report no. HEL 23-1, November.
- Morton, B.R., Taylor, G., and Turner, J.S. 1956. "Turbulent Gravitational Convection from Maintained and Instantaneous Sources," *Proceedings of the Royal Society of London*, Series A, Vol. 234, pp. 1-23.
- Munro, D. 1981. "Sea Water Exclusion from Tunneled Outfalls Discharging Sewage," *Report 7-M*, Water Research Centre, Stevenage Laboratory.
- Munro, D., Mollowney, B.M. 1974. The Effect of a Bottom Counter-current and Vertical Diffusion on Coliform Concentrations at the Shore Due Mainly to Wind-induced Onshore Currents. *Rapports et Proces-verbaux des Reunions Conseil international pour l'Exploration de la Mer* 167: 37-40.
- Papanicolaou, P.N. 1984. "Mass and momentum transport in a turbulent buoyant vertical axisymmetric jet", Ph.D. thesis, W.M. Keck Laboratory of Hydraulic and Water Resources, California Institute of Technology, Pasadena, California, U.S.A.
- Rawn, A.M., and Palmer, H.K. 1930. "Predetermining the Extent of a Sewage Field in

- Sea Water," *Proceedings of the American Society of Civil Engineers*, Vol. 94, pp. 1036-1046.
- Rawn, A.M., Bowerman, F.R., and Brooks, N.H. 1960. "Diffusers for Disposal of Sewage in Sea Water," *Proceedings of the American Society Civil Engineers*, Vol. 86, no. SA2, pp. 65-107.
- Richardson, L.F. 1926. "Atmospheric Diffusion on a Distance Neighbour Graph," *Proceedings of the Royal Society of London, Series A*, Vol. 110, pp. 709-737.
- Roberts, P.J.W., and Snyder, W.H. 1993. "Hydraulic Model for Boston Outfall. I: Riser Configuration," *Journal of Hydraulic engineering*, Vol. 119, No. 9, pp. 970-987.
- Rouse, H., Yih, C.S., and Humphreys, H.W. 1952. "Gravitational Convection from a Boundary Source," *Sortoyk ur Tellus*, Vol. 4, No. 3, pp. 201-210.
- Schmidt, W. 1941. "Turbulente Ausbreitung Eines Stromes Erhitzter Luft," *Zeitschr. Angew. Math and Mechanics*, Vol. 21, pp. 265-274.
- "Secondary treatment facilities plan." 1988. *Effluent outfall*, Vol. 5, Massachusetts Water Resources Authority, Boston, Mass.
- Sharp, J.J. 1968. Discussion of "Disposal of Sewage from Seaside Towns," by Wooland, P.J. and Ricketts, C.F., *Journal of Institution of Public Health Engineers*, February, pp. 33-39.
- Sharp, J.J. 1986. "The Effect of Waves on Buoyant Jets," *Proceedings of Institution of Civil Engineers*, Part 2, Vol. 81, September, pp. 471-475.
- Sharp, J.J. 1990. "The Use of Ocean Outfalls for Effluent Disposal in Small Communities and Developing Countries," *Water International*, Vol 15, pp. 35-43.

- Sharp, J.J., and Moore, E. 1987. "Estimation of Dilution in Buoyant Effluents Discharged into a Current," *Proceedings of the Institution of Civil Engineers, Part 2, Vol. 83, March*, pp. 181-196.
- Sharp, J.J., and Wang, C.S. 1974. "Arrested Wedge in Circular Tube." *Proc. ASCE. J. Hydraulics Division*, Vol. 100, pp. 1085-1088.
- Shuto, N., and Ti, L.H. 1974. "Wave Effects on Buoyant Plumes," *14th International Conference on Coastal Engineering, Denmark*, No. 3, pp. 2199-2208.
- Wilkinson, D.L. 1984. "Purging of Saline Wedges from Ocean Outfalls," *Journal of Hydraulic engineering*, Vol. 110, No. 12, pp. 1815-1829.
- Wilkinson, D.L. 1985. "Seawater Circulation in Sewage Outfall Tunnels," *Journal of Hydraulic engineering*, Vol. 111, No. 5, pp. 846-858.
- Wilkinson, D.L. 1988. "Hydraulic modeling of tunneled outfalls," *Proc. Int'l Conf. on Marine Disposal of Wastewater*, Wellington, New Zealand.
- Wilkinson, D.L. 1991. "Model Scaling Laws for Tunnel of Ocean-Sewage Outfalls," *Journal of Hydraulic engineering*, Vol. 117, No. 5, pp. 547-561.
- Wilkinson, D.L., and Nittim, R. 1992. "Model Studies of Outfall Riser Hydraulics," *Journal of Hydraulic Research*, Vol. 30, No. 5, pp. 581-593.
- Wood, I.R., Bell, R.G., and Wilkinson, D.L. 1993. "Ocean Disposal Wastewater," *World Scientific Publishing Co. Pte. Ltd., Singapore*.

APPENDIX A

Saline wedge profiles in tunnel with risers without caps

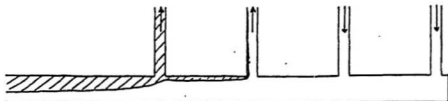


Figure A.1. Saline wedge profile in tunnel with risers without caps at effluent discharge
 $Q = 11.36$ l/min. and $\Delta\rho = 0.010$ g/cm³.

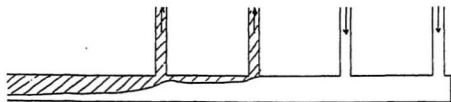


Figure A.2. Saline wedge profile in tunnel with risers without caps at effluent discharge
 $Q = 28.39$ l/min. and $\Delta\rho = 0.010$ g/cm³.

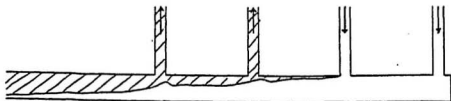


Figure A.3. Saline wedge profile in tunnel with risers without caps at effluent discharge
 $Q = 36.34$ l/min. and $\Delta\rho = 0.010$ g/cm³.

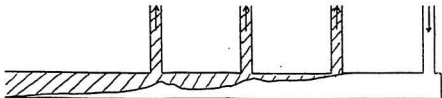


Figure A.4. Saline wedge profile in tunnel with risers without caps at effluent discharge $Q = 39.75$ l/min. and $\Delta\rho = 0.010$ g/cm³.

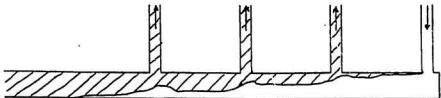


Figure A.5. Saline wedge profile in tunnel with risers without caps at effluent discharge $Q = 54.51$ l/min. and $\Delta\rho = 0.010$ g/cm³.

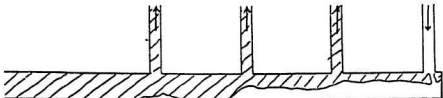


Figure A.6. Saline wedge profile in tunnel with risers without caps at effluent discharge $Q = 68.14$ l/min. and $\Delta\rho = 0.010$ g/cm³.

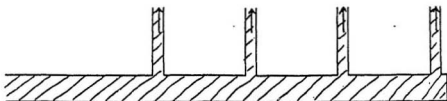


Figure A.7. Saline wedge profile in tunnel with risers without caps at effluent discharge
 $Q = 76.06 \text{ l/min.}$ and $\Delta\rho = 0.010 \text{ g/cm}^3$.

APPENDIX B

Saline wedge profiles in tunnel for different types of test

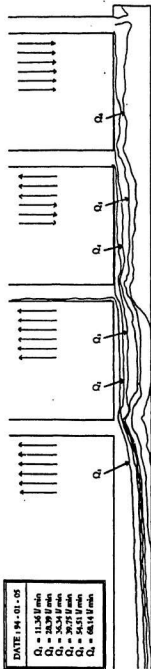


Figure B.1. Saline wedge profiles in tunnel with risers without cups at different freshwater discharges, and $\Delta\rho = 0.010 \text{ g/cm}^3$.

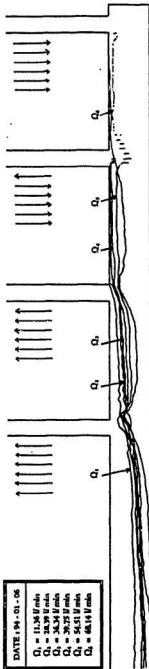


Figure B.2. Saline wedge profiles in tunnel with risers without cups at different freshwater discharges, and $\Delta\rho = 0.020 \text{ g/cm}^3$.

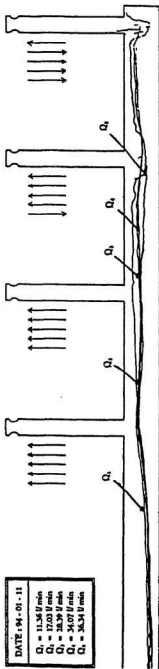


Figure B.3. Saline wedge profiles in tunnel with risers having caps with two ports at different freshwater discharges, and $\Delta\rho = 0.020 \text{ g/cm}^3$.

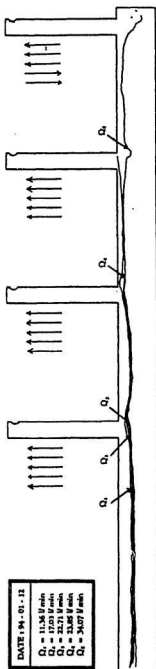


Figure B.4. Saline wedge profiles in tunnel with risers having caps with one port at different freshwater discharges, and $\Delta\rho = 0.020 \text{ g/cm}^3$.

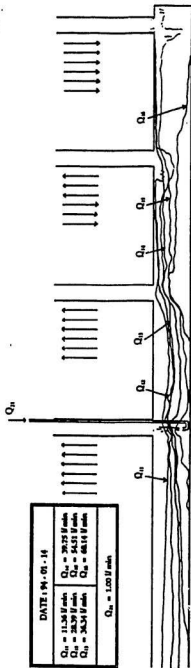


Figure B.5. Saline wedge profiles in tunnel with water jet located at first riser ($Q_{d1} = 1.00$ l/min), at different freshwater discharges, and $\Delta\rho = 0.010$ g/cm³.

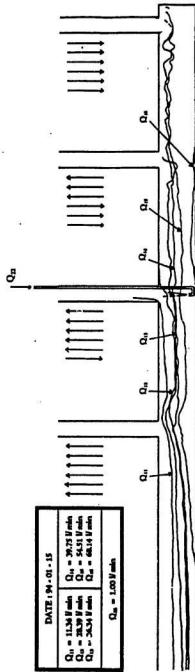


Figure B.6. Saline wedge profiles in tunnel with water jet located at second riser ($Q_{d2} = 1.00$ l/min), at different freshwater discharges, and $\Delta\rho = 0.010$ g/cm³.

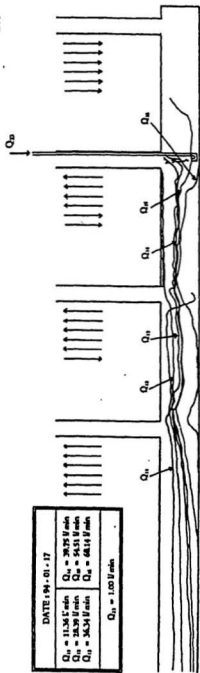


Figure B.7. Saline wedge profiles in tunnel with water jet located at third riser ($Q_{w3} = 1.00$ l/min), at different freshwater discharges, and $\Delta\rho = 0.010 \text{ g/cm}^3$.

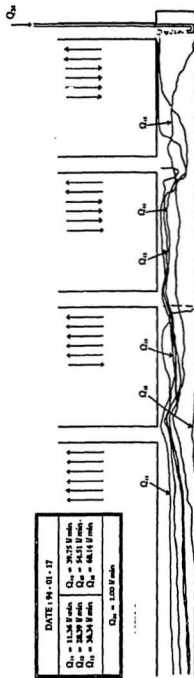


Figure B.8. Saline wedge profiles in tunnel with water jet located at fourth riser ($Q_{w4} = 1.00$ l/min), at different freshwater discharges, and $\Delta\rho = 0.010 \text{ g/cm}^3$.

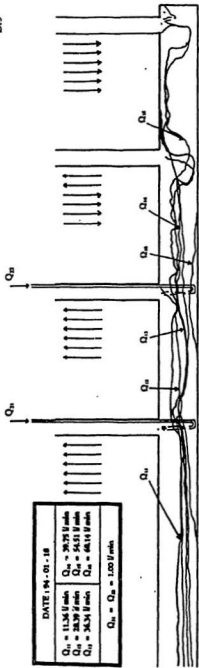


Figure B.9. Saline wedge profiles in tunnel with water jets located at first and second risers ($Q_{21} = Q_{22} = 1.00 \text{ l/min}$), at different freshwater discharges, and $\Delta\rho = 0.010 \text{ g/cm}^3$.

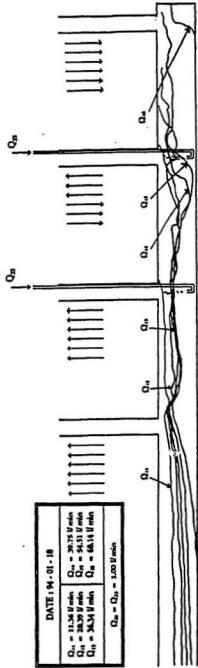


Figure B.10. Saline wedge profiles in tunnel with water jets located at second and third risers ($Q_{23} = Q_{33} = 1.00 \text{ l/min}$), at different freshwater discharges, and $\Delta\rho = 0.010 \text{ g/cm}^3$.

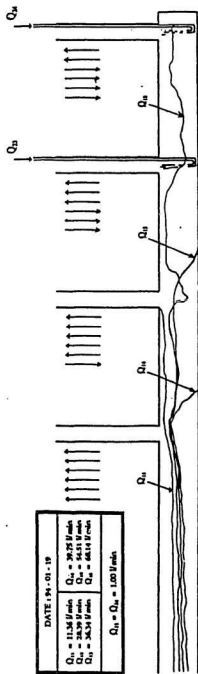


Figure B.11. Saline wedge profiles in tunnel with water jets located at third and fourth risers ($Q_{23} = Q_{24} = 1.00 \text{ l/min}$), at different freshwater discharges, and $\Delta\rho = 0.010 \text{ g/cm}^3$.

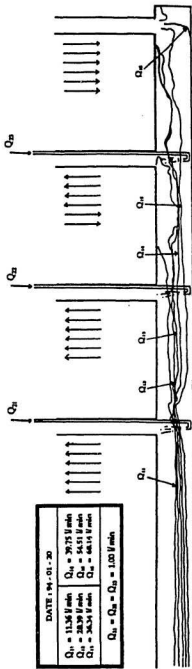


Figure B.12. Saline wedge profiles in tunnel with water jets located at first, second and third risers ($Q_{21} = Q_{22} = Q_{23} = 1.00 \text{ l/min}$), at different freshwater discharges, and $\Delta\rho = 0.010 \text{ g/cm}^3$.

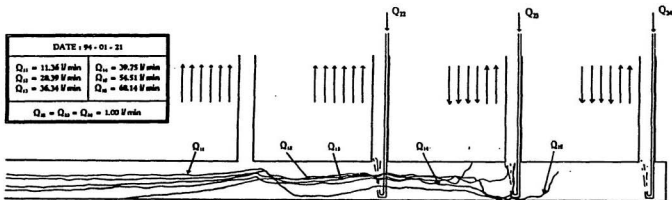


Figure B.13. Saline wedge profiles in tunnel with water jets located at second, third and fourth risers ($Q_{22} = Q_{23} = Q_{24} = 1.00 \text{ l/min}$), at different freshwater discharges, and $\Delta\rho = 0.010 \text{ g/cm}^3$.

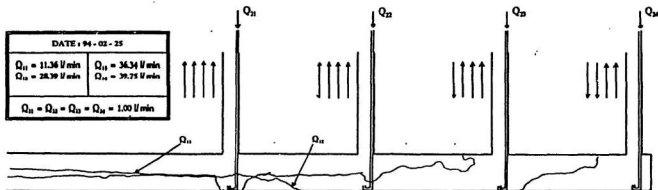


Figure B.14. Saline wedge profiles in tunnel with water jets located at first, second, third and fourth risers ($Q_{21} = Q_{22} = Q_{23} = Q_{24} = 1.00 \text{ l/min}$), at different freshwater discharges, and $\Delta\rho = 0.010 \text{ g/cm}^3$.

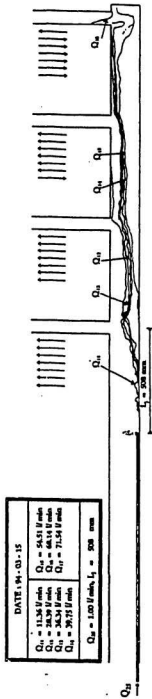


Figure B.15. Saline wedge profiles in tunnel with water jet located upstream of first riser (Q_{18} = 1.00 l/min), at different freshwater discharges, L_1 = 508 mm, and $\Delta\rho$ = 0.010 g/cm³.

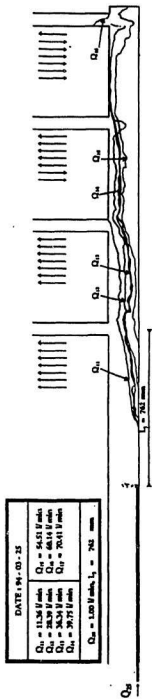


Figure B.16. Saline wedge profiles in tunnel with water jet located upstream of first riser (Q_{18} = 1.00 l/min), at different freshwater discharges, L_1 = 762 mm, and $\Delta\rho$ = 0.010 g/cm³.

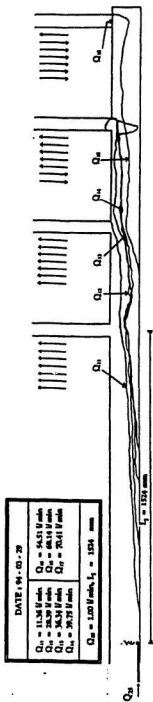


Figure B.17. Saline wedge profiles in tunnel with water jet located upstream of first riser ($Q_{10} = 1.00 \text{ l/min}$), at different freshwater discharges, $L_1 = 1574 \text{ mm}$, and $\Delta\rho = 0.010 \text{ g/cm}^3$.

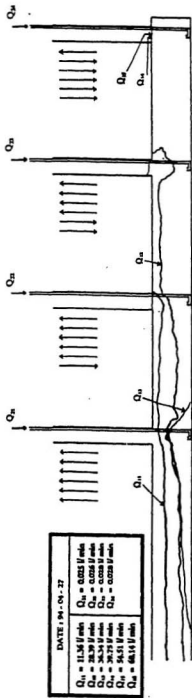


Figure B.18. Saline wedge profiles in tunnel with air jets located at first, second, third and fourth risers ($Q_{1a} = 0.025$ l/min, $Q_{2a} = 0.025$ l/min, $Q_{3a} = 0.028$ l/min, and $Q_{4a} = 0.028$ l/min), at different freshwater discharges, and $\Delta\rho = 0.010$ g/cm³.

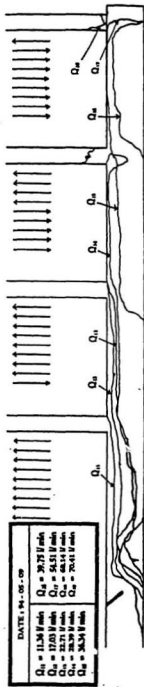


Figure B.19. Saline wedge profiles in tunnel with top barrier located upstream of first riser at different freshwater discharges, and $\Delta\rho = 0.010$ g/cm³.



